REPORT DOCUMENTATION PAGE

Form Approved
OMB NO. 0704-0188

1. AGENCY USE ONLY (Leave Blank)	2. REPORT DATE	3. REPORT TYPE AND DATES COVERED
	October 17, 2005	Final; 9/1/2002-8/30/2005

4. TITLE AND SUBTITLE

Rare Earth doped Semiconductors for Phosphors and Lasers

5. FUNDING NUMBERS

DAAD19-02-1-0316

6. AUTHOR(S)
Uwe Hommerich

7. PERFORMING ORGANIZATION NAME(S) AND ADDRESS(ES)

Hampton University, Department of Physics, Hampton, VA 23666

8. PERFORMING ORGANIZATION REPORT NUMBER

9. SPONSORING / MONITORING AGENCY NAME(S) AND ADDRESS(ES)

U. S. Army Research Office
P.O. Box 12211
Research Triangle Park, NC 27709-2211

10. SPONSORING / MONITORING AGENCY REPORT NUMBER

43798.1-EL-H

11. SUPPLEMENTARY NOTES

The views, opinions and/or findings contained in this report are those of the author(s) and should not be construed as an official Department of the Army position, policy or decision, unless so designated by other documentation.

12 a. DISTRIBUTION / AVAILABILITY STATEMENT

Approved for public release; distribution unlimited.

12 b. DISTRIBUTION CODE

13. ABSTRACT (Maximum 200 words)

The emission properties of rare earth (RE) doped III-nitrides remain of significant current interest for applications in display technology, optical communications, and solid-state lasers. Full-color displays based on RE doped GaN/AlGaN films have been developed by collaborators at the University of Cincinnati (Prof. A. Steckl group). In addition, the first demonstration of laser activity from GaN: Eu was recently reported indicating the potential of this novel class of materials as solid-state gain media.

In this final report, laser spectroscopic studies of the visible and infrared emission properties of GaN: Eu, GaN: Er, and AlGaN: Tm thin-films are presented. Collaborators at the University of Cincinnati prepared the investigated samples using solid-source MBE. Time-resolved and steady state photoluminescence studies were performed on RE doped GaN/AlGaN films in order to gain a better understanding on the RE incorporation, excitation mechanisms, and emission efficiency. The RE emission properties were investigated as a function of excitation wavelength, temperature, host composition (e.g. Tm: AlGaN), growth conditions (e.g. Ga-flux dependence of Er: GaN), and growth method (e.g. IGE growth of Eu: GaN). Initial studies of Er doped III-Nitride double heterostructures grown at Kansas State University are also summarized.

14. SUBJECT TERMS

III-Nitride semiconductor, Rare Earth Spectroscopy, Photoluminescence; Light emitting diodes

15. NUMBER OF PAGES

16. PRICE CODE

17. SECURITY CLASSIFICATION OR REPORT	18. SECURITY CLASSIFICATION ON THIS PAGE	19. SECURITY CLASSIFICATION OF ABSTRACT	20. LIMITATION OF ABSTRACT
UNCLASSIFIED	**UNCLASSIFIED**	**UNCLASSIFIED**	**UL**

NSN 7540-01-280-5500

Standard Form 298 (Rev.2-89)
Prescribed by ANSI Std. 239-18
298-102

RARE EARTH DOPED SEMICONDUCTORS FOR PHOSPHORS AND LASERS

FINAL PROGRESS REPORT

Uwe Hömmerich

October 17, 2005

U.S. ARMY RESEARCH OFFICE

GRANT DAAD19-02-1-0316

HAMPTON UNIVERSITY

TABLE OF CONTENTS

BODY OF REPORT

A. STATEMENT OF THE PROBLEM STUDIED

Rare Earth doped III-nitrides have emerged as a new class of luminescent materials for applications in display technology, optical communications, and solid-state lasers [1-15]. Electroluminescence (EL) devices have been fabricated at the University of Cincinnati (Prof. Steckl's group), which produced a luminance of ~1000 cd/m^2 at an efficiency of ~0.15 lm/W [16]. Very recently, the first demonstration of laser activity from GaN: Eu under optical pumping was reported indicating the potential of RE doped nitrides for solid-state laser applications [17].

The recent success in the development of RE doped nitrides light sources is intimately tied to systematic investigations on the optimization of the material synthesis and optical properties of RE ions [1-15]. As photoluminescence (PL) investigations performed under this award have shown, RE ions tend to occupy multiple sites within the nitride host material, which exhibit different excitation and de-excitation pathways. Optimization studies of Er doped GaN thin-films revealed, that the incorporation and excitation of Er^{3+} ions is strongly influenced by the gallium (Ga) flux employed during MBE growth. The EL and PL emission intensities from Er doped GaN films were maximum for materials grown under slightly nitrogen-rich growth condition. On the contrary, high quality GaN films are typically grown under Ga-rich growth condition. The complimentary behavior of intrinsic GaN bandedge emission and RE emission indicated the competition between carrier recombination processes and Er excitation efficiency. The red emission from Eu doped GaN was further investigated during the course of this work for new samples grown by conventional MBE and interrupted growth epitaxy (IGE). GaN: Eu grown using IGE technique exhibited improvement in the EL device performance by more then an order of magnitude compared to conventional MBE. During IGE the Ga shutter is closed for a certain time interval, which allows the GaN: Eu film to compensate for any nitrogen deficiency. An important optimization parameter for the blue emission from Tm doped nitrides was the bandgap energy of the host material. The blue emission from GaN: Tm was very weak due to a poor excitation efficiency. A careful study of the blue emission from Tm for a series of AlGaN samples revealed an improved excitation efficiency for larger bandgap energies of the host. The highest Tm emission intensity was observed for an $Al_xGa_{1-x}N$: Tm film with x~0.6. The obtained results demonstrated that the excitation process of RE ions in nitrides can be optimized through bandgap engineering of the host.

In this final report, the most important results of laser spectroscopic studies of GaN: Er, AlGaN:Tm, and GaN: Er prepared by solid-source MBE are summarized. In addition, some results of emission studies of Er doped III-N heterostructures are also discussed. More detailed information on the performed research can be found in the attached manuscripts.

B. SUMMARY OF MOST IMPORTANT RESEARCH RESULTS

The research performed under this grant has lead to 15 presentations at conferences and workshops. Moreover, the results were discussed in 6 refereed journal publications. The manuscripts are attached to this final report. In the following the most important research results are briefly summarized:

1. Emission properties of Er doped GaN as a function of Ga-flux during solid-source MBE growth

The optimization of the green and 1.54 μm emission properties of Er doped GaN are critical for the improvement of current EL devices for display applications and optical communications [1-5]. A careful study of the emission properties for varying growth conditions was performed at the University of Cincinnati and the samples were investigated for their emission properties at Hampton University. As was previously reported [18], the green ($^2H_{11/2}$, $^4S_{3/2}$->$^4I_{15/2}$) and infrared PL properties of Er^{3+} ions in GaN are strongly dependent on the Ga-flux used during MBE growth. During the time period of this award, we have extended these investigations to a comparison of the Er^{3+} PL properties for above- and below-gap pumping. Similar to above-gap excitation, the visible (green) and infrared (1.5 μm) Er^{3+} PL intensities are strongest for slightly N-rich growth conditions when pumped resonantly at 496.5 nm (i.e. below the bandgap of GaN).

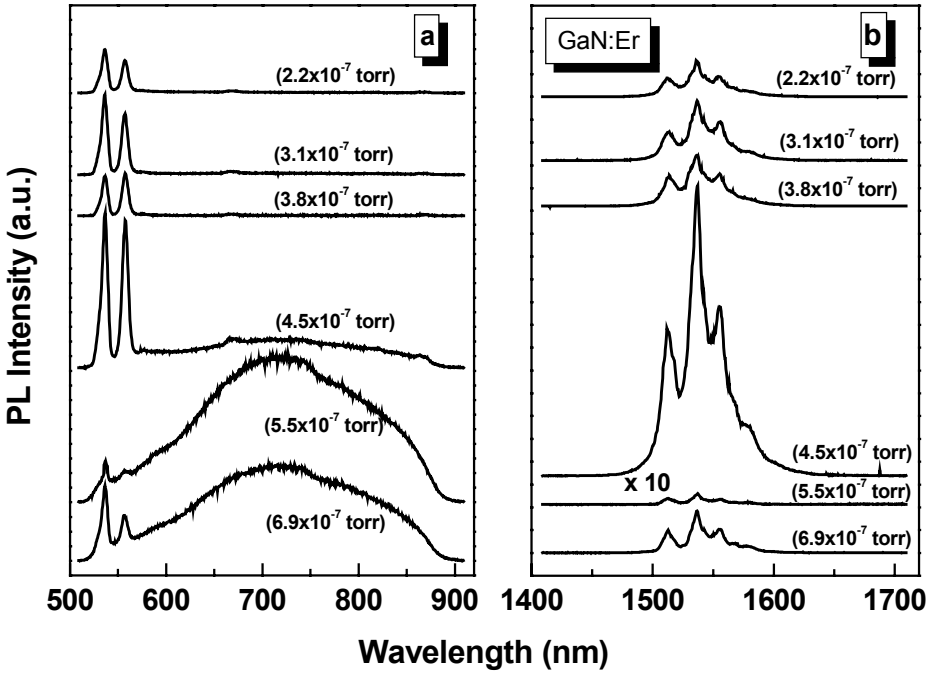

Figure 1: *Visible (a) and infrared (b) emission from Er doped GaN as a function of Ga-flux under below-gap excitation (496.5 nm). The Er^{3+} emission intensity reached its maximum under slightly N-rich flux near the stoichiometric growth condition (Ga-flux: ~4.5x10^{-7} torr) [18].*

Based on high-resolution PL and pump-power dependent PL studies, we concluded that the Er^{3+} incorporation and the concentration of optically active Er ions strongly dependent on the Ga-flux. Low temperature, high-resolution PL measurements revealed significant spectral changes of the 1.5 μm Er^{3+} PL for

samples grown with different Ga-fluxes. Moreover, PL saturation experiments revealed that only a small fraction (<10%) of the total Er ions in GaN are optically active for samples grown under Ga-rich conditions. The low optical activation of Er^{3+} ions in GaN is similar to recent observations made for Er doped Si/amorphous Si [19]. The optimization of the optically active concentration of Er^{3+} ions remains an important parameter, which can lead to a significant improvement of Er doped GaN based EL devices.

2. Spectroscopic studies of the visible and infrared emission of Tm doped AlGaN thin films

Visible emission studies of GaN/AlGaN: Tm

One of the main challenges in using RE doped GaN for full-color display applications has been obtaining efficient blue emission [1-5]. Previous studies have shown only weak blue emission from Tm doped GaN films [20]. During the time span of this grant, we have investigated PL properties of Tm^{3+} ions in a series of Tm doped $Al_xGa_{1-x}N$ films ($0 \le x \le 1$) grown by solid-source molecular-beam epitaxy. It was found that the blue PL properties of $Al_xGa_{1-x}N$: Tm vary significantly as a function of Al content (fig.2) [21].

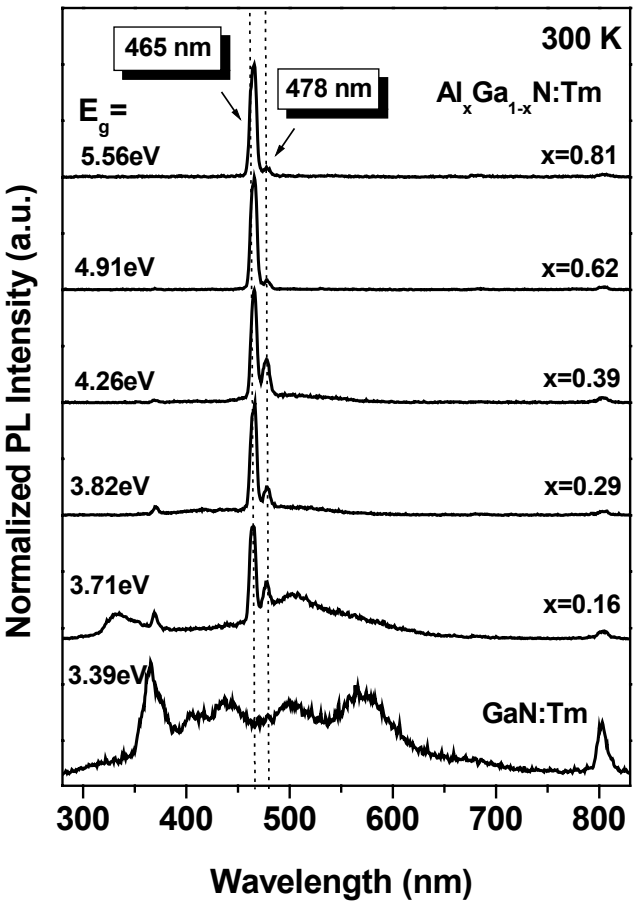

Figure 2: *Room temperature PL spectra of $Al_xGa_{1-x}N$: Tm excited at 250 nm. The dotted lines indicate the position of the blue PL arising from the transitions $^1G_4 \rightarrow {}^3H_6$ (~478 nm) and $^1D_2 \rightarrow {}^3F_4$ (~465 nm). The calculated bandgap energies (E_g) are also indicated in the figure.*

Under above-gap pumping, GaN:Tm exhibited a weak blue emission at ~478 nm from the $^1G_4$ -> $^3H_6$ transition of Tm^{3+}. With increasing Al content an enhancement of the blue PL at 478 nm was observed. In addition, an intense new blue PL line appeared at ~465 nm, which is assigned to the $^1D_2$ -> $^3F_4$ transition of Tm^{3+}. The overall blue PL intensity reached a maximum for x=0.62, with the 465 nm line dominating the visible PL spectrum. Under below-gap pumping, AlN: Tm also exhibited intense blue PL at 465 nm and 478 nm as well as several other PL lines ranging from the ultraviolet to near-infrared. The Tm^{3+} PL from AlN: Tm was most likely excited through defect-related complexes in the AlN host.

Infrared emission properties of GaN: Tm/AlGaN: Tm

In this study, the infrared (IR) emission properties of in-situ Tm doped $Al_xGa_{1-x}N$ thin films ($0 \le x \le 1$) prepared by solid-source molecular-beam epitaxy were investigated. Earlier work on IR studies of RE doped semiconductors was mainly focused on the 1.54 μm emission from Er^{3+} ions due to the overlap with the minimum loss window of silica based fibers [1-5]. The growing demand for increased bandwidth of optical communication systems has prompted efforts to study the IR emission from other RE ions such as Dy^{3+} (1.3 μm), Pr^{3+} (1.3, 1.6 μm), Nd^{3+} (1.3 μm), and Tm^{3+} (1.48 μm). Tm^{3+} is currently considered the most promising candidate for S-band optical amplifiers, which cover a wavelength range from 1450 to 1530 nm [22].

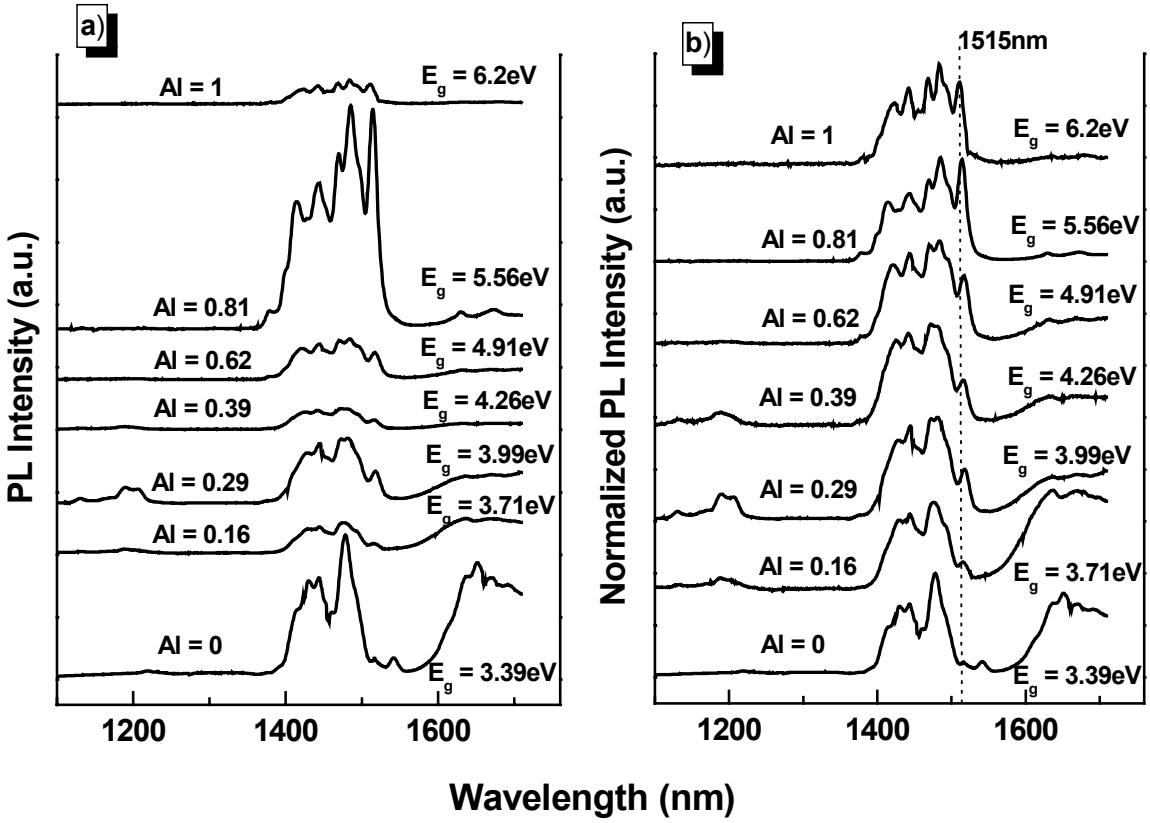

Figure 3: *a) Infrared PL spectra of $Al_xGa_{1-x}N$:Tm films at 300K showing the intensity changes as a function of Al content. b) Normalized IR PL of $Al_xGa_{1-x}N$:Tm for direct comparison of spectral changes [23].*

As depict in figure 3, all AlGaN: Tm samples exhibited 1.48 μm photoluminescence (PL) from the $^3H_4 \rightarrow {}^3F_4$ transition of Tm^{3+}. The PL spectra were measured using the UV Argon laser lines (333.6-363.8) nm, which corresponds to below-gap excitation for $Al_xGa_{1-x}N$ samples with x > 0 and above-gap pumping for x = 0 (GaN). Besides 1.48 μm PL, IR emission bands centered around 1.2 μm and 1.7 μm were observed, which can be assigned to the intra-4f transitions $^3H_5 \rightarrow {}^3H_6$ and $^3F_4 \rightarrow {}^3H_6$ of Tm^{3+} ions, respectively. The absolute intensity of the 1.48 μm PL varied strongly with Al content and reached a maximum for $Al_{0.81}Ga_{0.19}N$:Tm. The integrated 1.48 μm PL from $Al_{0.81}Ga_{0.19}N$: Tm was only weakly temperature dependent and decreased by less than a factor of two between 15 K and 300 K. The PL lifetime of the $^3H_4$ state decreased only slightly from ~102 μs to ~86 μs for the same temperature range. The results suggest that non-radiative decay processes in the $^3H_4$ level are small in $Al_{0.81}Ga_{0.19}N$: Tm, which is supported by the well-known energy-gap law for multiphonon relaxations. The initial studies indicate the potential of AlGaN: Tm films for electroluminescence device applications in the S-band optical communications window.

3. Photoluminescence studies of Eu doped GaN prepared by MBE and interrupted growth epitaxy (IGE)

Red emission properties of GaN: Eu prepared by conventional MBE technique

During the time-period of this report, we focused on high-resolution PL and PL excitation studies on Eu doped GaN films prepared by solid-source MBE in order to gain more insight into the incorporation and excitation process of Eu^{3+} ions. A survey high-resolution PL spectrum of Eu doped GaN is shown in fig. 4.

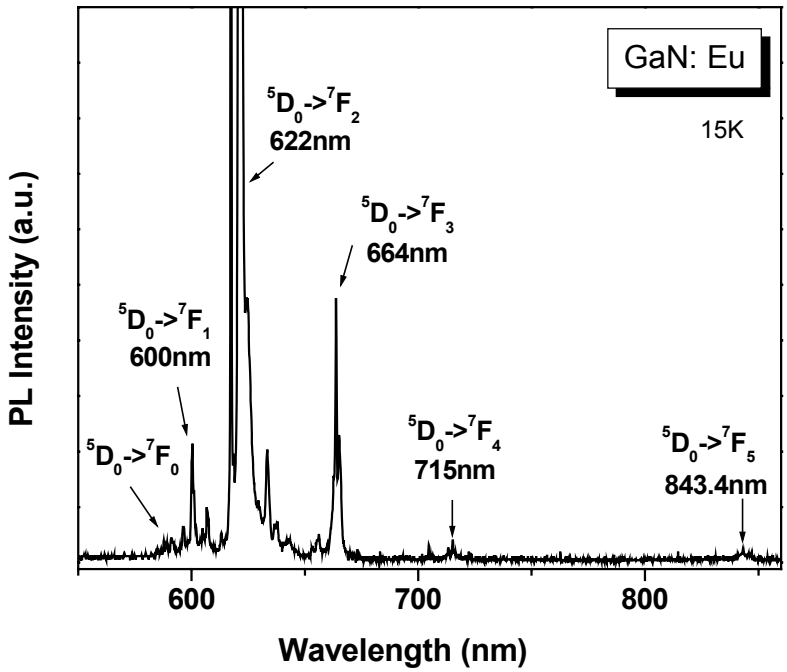

Figure 4: *Emission spectrum of GaN:Eu at 15K under above-gap excitation. The main emission features arising from the $^5D_0 \rightarrow {}^7F_J$ (J=0,1,2,3,4,5) transitions are indicated in the graph.*

The main emission lines can be assigned to the transitions: $^5D_0$ -> $^7F_5$ (~843 nm), $^5D_0$ -> $^7F_4$ (~715 nm), $^5D_0$ -> $^7F_3$ (~664 nm), $^5D_0$ ->$^7F_2$ (~622 nm), and $^5D_0$ -> $^7F_1$ (~600 nm). The weak emission features at ~585 nm and ~590 nm are most likely due to $^5D_0$ -> $^7F_0$ transitions suggesting multiple Eu^{3+} centers in GaN. In order to identify the $^5D_0$ <-> $^7F_0$ transitions and associated Eu^{3+} centers more clearly, we have performed high-resolution PL excitation (PLE) studies in the range from 560-595 nm (see fig. 5). At low temperature (15 K) five PLE lines at 571 nm, 585.8 nm, 587.9 nm, 588.9 nm, and 589.4 nm were observed and tentatively assigned to $^7F_0$ -> $^5D_0$ transitions. We concluded that at least five different Eu^{3+} centers exist in GaN: Eu, which can be grouped into three dominant sites being optically excitable at ~571nm, ~586 nm, and 589 nm.

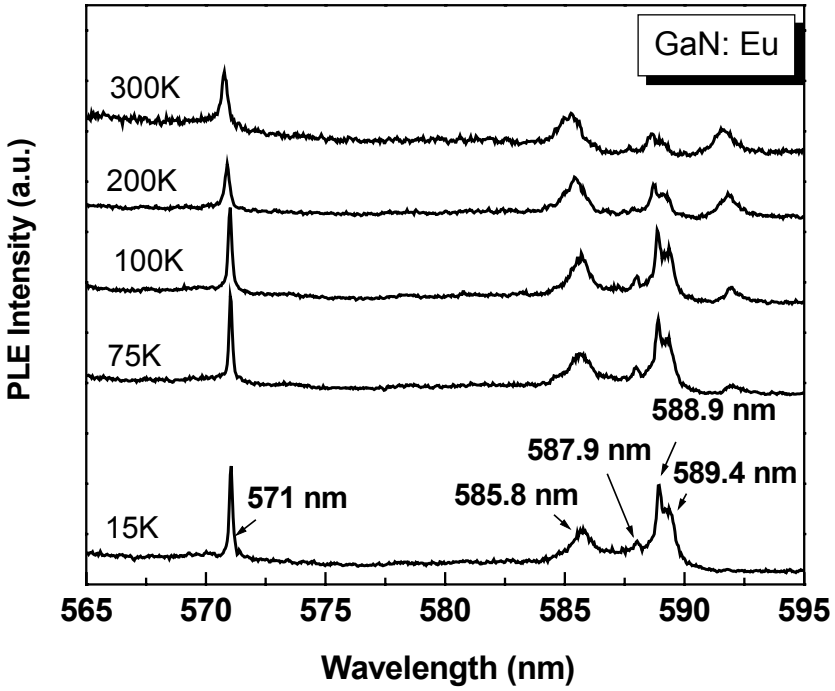

Figure 5: *High-resolution PLE spectrum of Eu doped GaN at 15 K. The emission was monitored at ~623 nm. $^7F_0$-$^5D_0$ absorption lines located at 571 nm, 585.5 nm, 587.9 nm, 588.9 nm, and 589.4 nm can be identified.*

More support for the identification of the different Eu^{3+} centers was obtained from site-selective PL measurements (fig. 6). Pumping resonantly into each of the PLE line revealed different Eu^{3+} emission spectra and lifetimes. The spectral differences are especially pronounced for the Eu^{3+} center excited at 571 nm. It can be speculated that the 571 nm center is associated with Eu^{3+} ions in substitutional Ga^{3+} lattice positions, whereas the other Eu^{3+} centers are due to Eu^{3+} ions incorporated into interstitial sites with close vicinity to other defects and impurities. Interestingly, the PL spectrum excited at 571 nm is very similar to PL spectra obtained under above-gap pumping, which shows that this Eu^{3+} center dominates under carrier-mediated excitation.

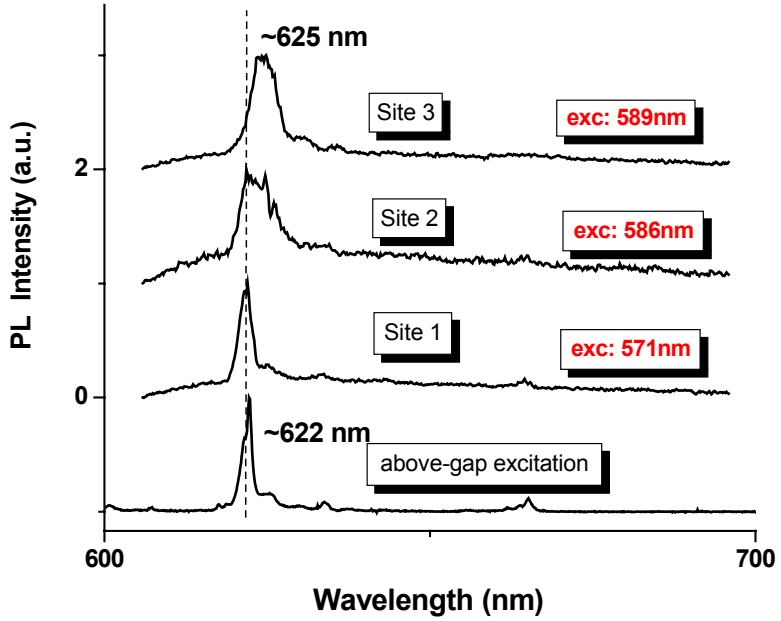

Figure 6: PL excitation spectrum of GaN: Eu grown by SSMBE.

Red emission properties of GaN: Eu prepared by interrupted growth epitaxy (IGE) technique

In an effort to further improve the overall red emission from GaN: Eu, a new set of samples was grown at the University of Cincinnati using the technique of interrupted growth MBE [16]. The motivation behind this study was to investigate the effect of the III-V ratio on the Eu^{3+} emission properties in Eu doped GaN. Fig. 7 shows an overview of the room-temperature PL spectra of Eu doped GaN for various Ga shutter cycling times.

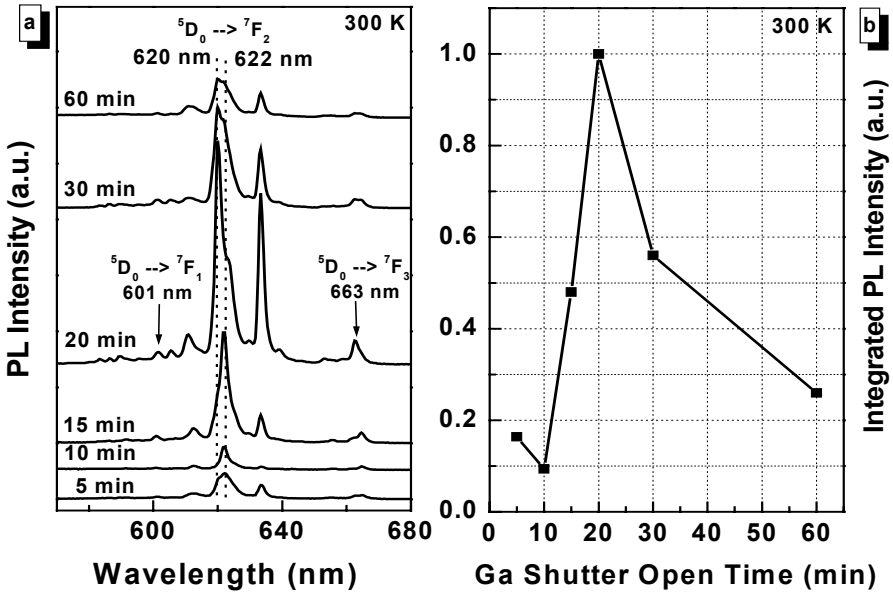

Figure 7. *(a) Room temperature PL spectra of GaN:Eu films under above-gap excitation. The group III shutter open times are also indicated in the graph. (b) Integrated PL intensity of GaN:Eu films as a function of Ga/Eu shutter cycling time.*

The PL was excited using an UV argon laser (333.6-363.8 nm), which corresponds to above-gap pumping. The characteristic Eu^{3+} red emission at ~ 622 nm attributed to the intra-4f $^5D_0 \rightarrow {}^7F_2$ transition was observed in all samples accompanied by other Eu^{3+} lines at ~ 601 nm ($^5D_0 \rightarrow {}^7F_1$) and ~ 663 nm ($^5D_0 \rightarrow {}^7F_3$). The strongest red emission was observed from GaN:Eu with a shutter cycling time of 20 min as illustrated in Fig. 7 (a). The integrated PL intensity as a function of Ga shutter cycling time is also depicted in Fig. 7 (b). It can be noticed from Fig. 7, that the main red emission line consisted of two peaks at ~ 620 nm and ~ 622 nm. The intensity ratio of these two PL lines changed as a function of Ga shutter cycling time. The GaN:Eu sample with the strongest Eu^{3+} PL intensity exhibited mainly emission from the 620 nm PL line. The observation of two strong $^5D_0 \rightarrow {}^7F_2$ PL lines suggests the existence of two dominant Eu^{3+} sites (labeled in figure 8 as site 1 and site 2). It is also interesting to note that the PL line at ~ 633 nm was unusually pronounced in some GaN:Eu samples, and was correlated with the 620 nm PL line intensity. The weak emission lines at 583, 586, and 589 nm are most probable due to $^5D_0 \rightarrow {}^7F_0$ transitions further indicating the existence of different Eu^{3+} centers in GaN:Eu samples grown by IGE technique.

To gain more insight in the Eu^{3+} PL properties of GaN:Eu prepared by IGE, PL spectra were recorded under resonant intra-4f Eu^{3+} excitation using the 471 nm output of an OPO system [Fig. 8 (a)]. Nearly identical Eu^{3+} PL spectra with the $^5D_0 \rightarrow {}^7F_2$ emission line at ~ 622 nm were observed for all samples. This observation suggests that Eu^{3+} site 2 is dominant under resonant pumping. The normalized PL spectra under above-gap excitation are shown in Fig. 8 (b) for comparison.

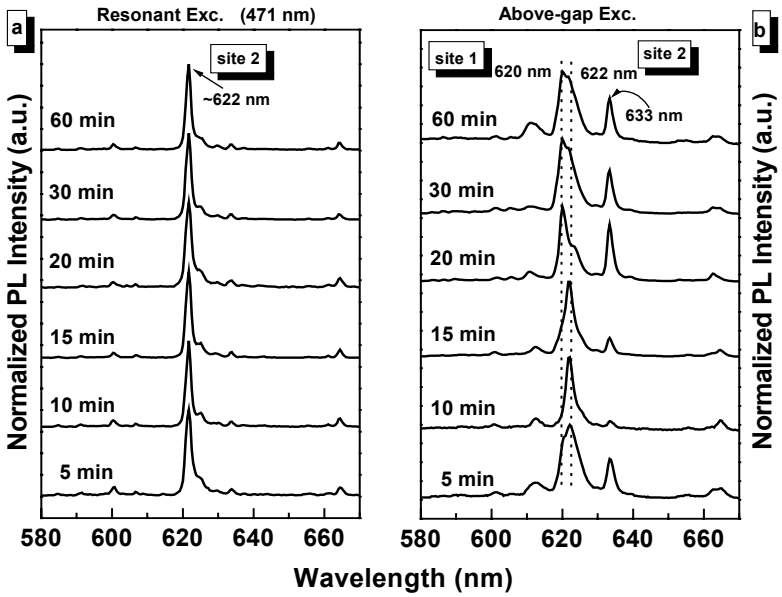

Figure 8. *Normalized PL spectra of GaN: Eu under (a) resonant and (b) above-gap excitation. The group III shutter open times during IGE growth are also indicated in the graph.*

The differences in PL spectra under above-gap and resonant-excitation further indicate that different Eu^{3+} centers were formed in GaN during the IGE growth process. Compared to above- gap excitation, resonant

Eu^{3+} excitation preferentially excited only one Eu^{3+} site (site 2). The PL decay monitored at ~ 622 nm under resonant-excitation showed that the transients are nearly exponential with variations in 1/e lifetimes ranging from ~ 100-215 μs. Overall, GaN:Eu samples grown by IGE technique provide great promise for improved EL device performance in display applications. Moreover, the recent observation of laser action from Eu doped GaN under optical excitation indicates the potential of this material for solid-state laser application [17]. The first realization of an electrically pumped RE doped semiconductor laser seems also possible using Eu doped GaN.

4. Electroluminescence and Photoluminescence studies of Er doped GaN hetrostructures

As part of a collaboration between the Army Research Office, SVT Associates, Kansas State University, and Hampton University, initial studies of Er-doped III-N double heterostructures (DHs), namely AlGaN/GaN:Er/AlGaN grown on sapphire, were performed. Compared to single heterostructures AlGaN/GaN:Er, the DHs films showed a significant enhanced 1.54 μm emission from Er^{3+} ions, suggesting a more efficient carrier confinement in the quantum well region (fig. 9) [24].

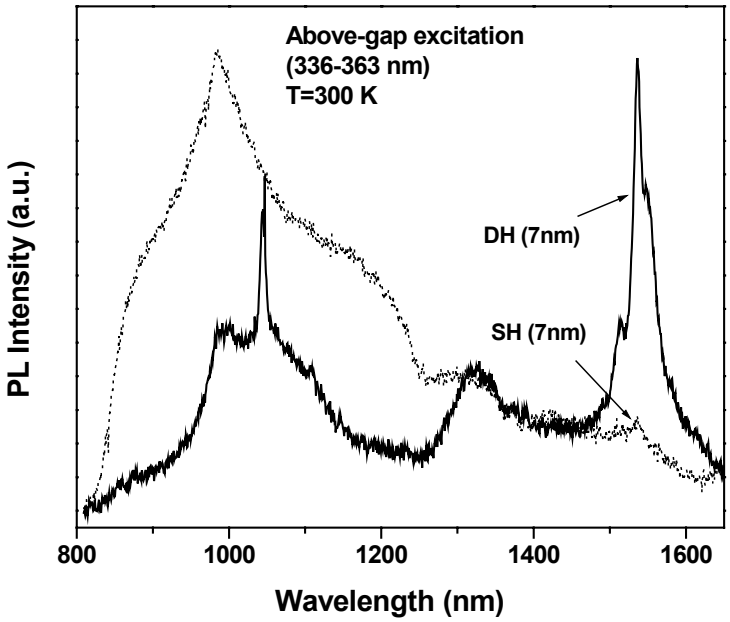

Figure 9. *Infrared PL spectra of a 7 nm GaN:Er/AlGaN SH (dotted line) and a 7 nm AlGaN/GaN:Er/AlGaN DH (solid line). The spectra were measured at 300 K using pump radiation at 336-363 nm.*

Some EL device performance studies of the quantum well like structures were also carried out Hampton University during time period of this grant (see fig. 10). 1.54 μm emission was observed under forward and reverse bias conditions. The EL intensity was slightly stronger under reversed biased excitation and the EL spectrum was significantly narrower. These results indicate that a different subset of Er^{3+} ions was electrically

excited depending on biasing conditions. Further optimization of the growth and device fabrication of these quantum well structures is needed to fully explore their potential for optoelectronic device applications.

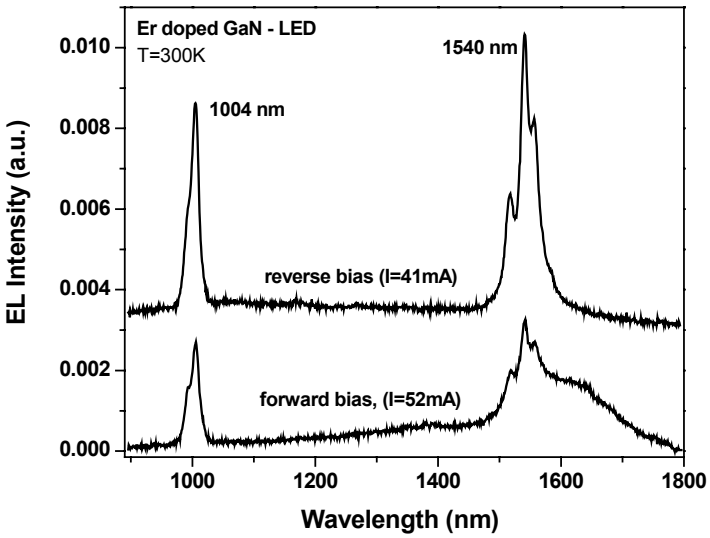

Figure 10. *Room temperature infrared EL spectra of the GaN:Er LED under forward and reverse bias excitation.*

C. LIST OF PUBLICATIONS AND TECHNICAL REPORTS

a) Papers published in peer-reviewed journals

E. Nyein, U. Hömmerich, D.S. Lee, A.J. Steckl, and J. M. Zavada, "Spectroscopic studies of the infrared emission from Tm doped AlGaN thin films", Phys. Stat. Sol. (C) 2 (2005) 2796.

U. Hömmerich, Ei Ei Nyein, D. S. Lee, A. J. Steckl, J. M. Zavada, "Photoluminescence Properties of in-situ Tm-doped AlGaN", Appl. Phys. Lett. 83, (2003), 4556-4558

U. Hommerich, EiEi Nyein, D. S. Lee, J. Heikenfeld, A. J. Steckl, and J. M. Zavada, "Photoluminescence Studies of Rare Earth (Er,Eu,Tm) in-situ doped GaN", Materials Science and Engineering B105, (2003) 91-96.

J. M. Zavada, J. Y. Lin, H. X. Jiang, P. Chow, B. Hertog, U. Hommerich, Ei Ei Nyein, and H. A. Jenkinson, "Synthesis and optical characterization of Erbium doped III-N Double Heterostructures, Materials Science and Engineering B105, (2003) 118-121.

J. M. Zavada, R. G. Wilson, U. Hommerich, M. Thaik, J. T. Seo, C. J. Ellis, J. Y. Lin, H.X. Jiang, "Compositional Changes in Erbium-Implanted GaN Films due to Annealing, Journal of Electronic Materials, Vol. 32, No.5 (2003) 382.

Ei Ei Nyein, U. Hommerich, A. J. Steckl, J.M. Zavada, "Spectral and Time-resolved Photoluminescence Studies of Eu doped GaN", Applied Physics Letters, 82, (2003), 1655-1657.

b) Paper published in non-peer reviewed journals or in conference proceedings

Ei Ei Nyein, Uwe Hömmerich, Chanaka Munasinghe, Andrew J. Steckl, and John M. Zavada, "Excitation-Wavelength Dependent and Time-Resolved Photoluminescence Studies of Europium Doped GaN Grown by Interrupted Growth Epitaxy (IGE)", Materials Research Society Proceedings, Vol. 866, Symposium V; Spring 2005, paper V3.5.

Chanaka Munasinghe, Andrew J. Steckl, Ei Ei Nyein, Uwe Hömmerich, Hongying Peng, Henry Everitt, Zack Fleischman, Volkmer Dierolf, and John M. Zavada, "GaN: Eu Interrupted Growth Epitaxy (IGE): Thin Film Growth and Electroluminescent Devices, Materials Research Society Proceedings, Vol. 866, Symposium V; Spring 2005, paper V3.1.

John M. Zavada, EiEi Nyein, U. Hommerich, K.H. Kim, J.Y. Lin, H. X. Jiang, P. Chow, B. Hertog, "Visible and Infrared Emission from Er-doped III-N Light Emitting Diodes, Materials Research Society Proceedings, Vol. 866, Symposium V; Spring 2005, paper V3.4.

Ei Ei Nyein, U. Hommerich, A. J. Steckl, J. M. Zavada, "Ultraviolet and blue emission properties of Tm doped AlGaN and AlN", Conference on Lasers and Electro-Optics/Quantum Electronics & Laser Science (CLEO/QELS), San Francisco, CA , May 18-20, 2004, Technical Digest, paper CWA27.

Ei Ei Nyein, U. Hömmerich, D. S. Lee, A. J. Steckl, J. M. Zavada.. Spectroscopic studies of GaN :Er, GaN:Eu and GaN/AlGaN:Tm prepared by Solid-Source MBE; Presented at the 16th Annual Laser and Electro Optics Society Meeting, Tucson, Arizona, October 26-30, 2003, Technical Program paper ThM2.

U. Hömmerich, Ei Ei Nyein, A. J. Steckl, D. S. Lee, J. Heikenfeld, J. M. Zavada, Photoluminescence studies of rare-earth (Er, Eu, Tm) doped GaN; European Materials Research Society Meeting 2003 (E-MRS 2003), Strasbourg, France, June 10-13, 2003, Technical Program, paper J-V.1.

J. M. Zavada, J. Y. Lin, H. X. Jiang, P. Chow, U. Hömmerich, Ei Ei Nyein, H. Jenkinson Synthesis and optical characterization of Erbium-doped AlGaN quantum wells; European Materials Research Society Meeting 2003 (E-MRS 2003), Strasbourg, France, June 10-13, 2003, Technical Program, paper J-V.4.

Ei Ei Nyein, U. Hömmerich, A. J. Steckl, D. S. Lee, J. Heikenfeld, J. M. Zavada.Characterization of the red light emission from Eu-doped GaN; Conference on Lasers and Electro-Optics/Quantum Electronics & Laser Science (CLEO/QELS), Baltimore, MD, June 1-6, 2003, Technical Digest, paper CWA16.

c) Papers presented at meetings, but not published in conference proceedings

U. Hömmerich "Spectroscopic Studies of Eu doped GaN and Tm doped AlGaN", ARO Workshop on the Doping of III-N Semiconductors with Rare Earth and Transition Metals, Pittsburg, PA, July 20, 2004, oral presentation.

Ei Ei Nyein and U. Hömmerich, "Spectroscopic studies of the infrared emission from Tm doped AlGaN thin films", ARO Workshop on the Doping of III-N Semiconductors with Rare Earth and Transition Metals, Pittsburg, PA, July 20, 2004, oral presentation.

Ei Ei Nyein, U. Hömmerich, D.S. Lee, A.J. Steckl, and J. M. Zavada, "Spectroscopic studies of the infrared emission from Tm doped AlGaN thin films", presented at the International Workshop on Nitride Semiconductors, Pittsburg, PA, July 19-23, 2004, poster P 8.29.

D.S. Lee, A. J. Steckl, U. Hommerich, EiEi Nyein, J.M. Zavada, "Enhanced blue emission from Tm-doped AlGaN electroluminescent films, presented at the International Semiconductor Device Research Symposium (ISDRS), Washington, DC, Dec.10-12, 2003, paper WP1-03.

Ei Ei Nyein, U. Hömmerich, D. S. Lee, A. J. Steckl, J. M. Zavada, Photoluminescence properties of in-situ Tm doped $Al_xGa_{1-x}N$; "8th Wide-Bandgap III-Nitride Workshop", Omni Hotel, Richmond, Virginia, September 28-30, 2003.

Ei Ei Nyein, U. Hömmerich, D. S. Lee, A. Steckl, J. M. Zavada, "Spectroscopic studies of Erbium doped GaN as a function of Ga-flux; 'Impurity Based Electroluminescence in Wide Bandgap Semiconductors'; EL Workshop, The BISHOP'S LODGE, Santa Fe, NM, April 13-16, 2003.

U. Hömmerich, Ei Ei Nyein, D. S. Lee, J. Heikenfeld, A.J. Steckl, J. M. Zavada, Luminescence properties of rare-earth doped GaN; 'Impurity Based Electroluminescence in Wide Bandgap Semiconductors'; EL Workshop, The BISHOP'S LODGE, Santa Fe, NM, April 13-16, 2003.

d) Manuscript submitted, but not yet published

e) Technical reports submitted to ARO

Interims report 2003
Interims report 2004

D. SCIENTIFIC PERSONNEL

Senior Personnel

P.I., U. Hommerich	supported by this grant during summer 2003, 2004, and 2005.
J. T. Seo	supported by this grant during summer 2003
D. Temple	supported by this grant during summer 2005

Graduate Students

Ei Ei Nyein:	supported since fall 2003, received Ph.D. degree in Physics in May 2005
Ivy Krystal Jones	supported during summer 2005
Jessica Freeman	supported during spring and summer 2005
Peter Amedzake	supported during summer 2005

Undergraduate Student:

Osei Poku:	supported during Spring 2003, graduated in May 2004

INVENTIONS

none

BIBLIOGRAPHY

[1] S. Coffa, A. Polman, and R. N. Schwartz, (Eds.), *Rare Earth Doped Semiconductors II*, Materials Research Society, Vol. 422, 1996.

[2] A.J. Steckl and J.M. Zavada, MRS Bulletin, 24 (9) (1999) 33.

[3] J.M. Zavada, T. Gregorkiewicz, and A. J. Steckl, (Eds.), *Rare Earth Doped Semiconductors III,* Materials Science & Engineering B, Vol. 81, 2001.

[4] A. J. Steckl, J. C. Heikenfeld, D. S. Lee, M. J. Garter, C. C. Baker, Y. Wang, R. Jones, IEEE J. Sel. Top. Quant. **8**,749 (2002).

[5] *Rare Earth Doped Materials for Photonics,* Proceedings of E-MRS Symposium Spring 2003, (P. Ruterana, Editor.), Mater. Sci. Eng. **B105**, Elsevier (2003).

[6] Z. Li, H. Bang, G. Piao, J. Sawahata, K. Akimoto, J. Crystal Growth 240 (2002) 382.

[7] J. T. Torvik, C. H. Qui, R. J. Feuerstein, J. I. Pankove, and F. Namavar, J. Appl. Phys. 81 (1997) 6343.

[8] H. J. Lozykowski, W. M. Jadwisienczak, I.G. Brown, Appl. Phys. Lett. 74 (1999) 1129.

[9] E. Alves, M. F. da Silva, J. C. Soares, R. Vianden, J. Bartels, A. Kozanecki, Nucl. Instr. and Meth. B 147 (1999) 383.

[10] S. Kim, S. J. Rhee, X. Li, J. J. Coleman, S. G. Bishop, and P.B. Klein, J. Electron. Mater. 27 (1998) 246.

[11] S. Morishima, T. Maruyama, M. Tanaka, Y. Masumoto, K. Akimoto, Phys. Stat. Sol. A 176 (1999) 113.

[12] V. I. Dimitrova, P. G. Van Patten, H. H. Richardson, and M. E. Kordesh, Appl. Phys. Lett. 77 (2000) 478.

[13] T. Monteiro, C. Boemare, M. J. Soares, R. A. Sa Ferreira, L. D. Carlos, K. Lorenz, R. Vianden, E. Alves, Physica B 308-310 (2001) 22.

[14] U. Wahl, A. Vantomme, G. Langouche, J. P. Araujo, L. Peralta, J. G. Correia, and the ISOLDE collaboration, J. Appl. Phys. 88 (2000) 1319.

[15] H. J. Lozykowski, W. M. Jadwisienczak, J. Han, I.G. Brown, Appl. Phys. Lett. 77 (2000) 767.

[16] Chanaka Munasinghe, Andrew J. Steckl, Ei Ei Nyein, Uwe Hömmerich, Hongying Peng, Henry Everitt, Zack Fleischman, Volkmer Dierolf, and John M. Zavada, "GaN: Eu Interrupted Growth Epitaxy (IGE): Thin Film Growth and Electroluminescent Devices, Materials Research Society Proceedings, Vol. 866, Symposium V; Spring 2005, paper V3.1.

[17] J. H. Park, A. J. Steckl, Appl. Phys. Lett. 85, 4588 (2004).

[18] D.S. Lee, J. Heikenfeld, A.J. Steckl, U. Hömmerich, J. T. Seo, A. Braud, J. M. Zavada, Appl. Phys. Lett. 79, 719 (2001).

[19] O. B. Gusev, M. S. Bresler, P. E. Pak, I. N. Yassievich, M. Forcales, N. Q. Vinh, T. Gregorkiewicz, Phys. Rev. B 64 (2001) 075302.

[20] A. J. Steckl, M. Garter, D. S. Lee, J. Heikenfeld, and R. Birkhahn, Appl. Phys. Lett. **75,** 2184 (1999).

[21] U. Hömmerich, Ei Ei Nyein, D. S. Lee, A. J. Steckl, J. M. Zavada, Appl. Phys. Lett. 83, (2003), 4556-4558

[22] M. Yamada and M. Shimizu, NTT Technical Rev. **1**, 80 (2003).

[23] E. Nyein, U. Hömmerich, D.S. Lee, A.J. Steckl, and J. M. Zavada, Phys. Stat. Sol. (C) 2 (2005) 2796.

[24] J. M. Zavada, J. Y. Lin, H. X. Jiang, P. Chow, B. Hertog, U. Hommerich, Ei Ei Nyein, and H. A. Jenkinson, Materials Science and Engineering B105, (2003) 118-121.

Spectral and time-resolved photoluminescence studies of Eu-doped GaN

Ei Ei Nyein and U. Hömmerich[a)]
Department of Physics, Hampton University, Hampton, Virginia 23668

J. Heikenfeld, D. S. Lee, and A. J. Steckl
University of Cincinnati, Nanoelectronics Laboratory, Cincinnati, Ohio 45221

J. M. Zavada
US Army Research Office, Durham, North Carolina 27709

(Received 6 December 2002; accepted 20 January 2003)

We report on spectral and time-resolved photoluminescence (PL) studies performed on Eu-doped GaN prepared by solid-source molecular-beam epitaxy. Using above-gap excitation, the integrated PL intensity of the main Eu^{3+} line at 622.3 nm ($^5D_0 \rightarrow {}^7F_2$ transition) decreased by nearly 90% between 14 K and room temperature. Using below-gap excitation, the integrated intensity of this line decreased by only $\sim 50\%$ for the same temperature range. In addition, the Eu^{3+} PL spectrum and decay dynamics changed significantly compared to above-gap excitation. These results suggest the existence of different Eu^{3+} centers with distinct optical properties. Photoluminescence excitation measurements revealed resonant intra-4*f* absorption lines of Eu^{3+} ions, as well as a broad excitation band centered at ~ 400 nm. This broad excitation band overlaps higher lying intra-4*f* Eu^{3+} energy levels, providing an efficient pathway for carrier-mediated excitation of Eu^{3+} ions in GaN. © *2003 American Institute of Physics.* [DOI: 10.1063/1.1560557]

The visible and infrared light emissions from rare-earth-doped GaN (GaN:RE) are of significant current interest for applications in thin-film electroluminescence (EL) devices.[1–4] For achieving red light emission, the $^5D_0 \rightarrow {}^7F_2$ intra-4*f* transition of trivalent Eu^{3+} ions seems most promising. Intense red photoluminescence (PL) around 622 nm from GaN:Eu (as-grown and ion-implanted) has been reported from several research groups.[1–9] In addition, several EL device structures based on GaN:Eu have been demonstrated.[1–5] The optimization of present EL devices, however, requires a more detailed understanding of the incorporation, excitation, and emission properties of Eu^{3+} ions in the GaN host matrix.

Several studies have recently appeared focusing on the preparation and optical properties of GaN:Eu.[4–11] Based on the comparison to RE ions in other III–V semiconductors (e.g., InP:Yb,[12] GaAs:Er[13]), the most probable lattice location for Eu^{3+} ions in GaN are (substitutional) Ga sites, which have C_{3V} symmetry. However, significant differences in the Eu^{3+} PL properties have been observed depending on the material preparation. Monteiro *et al.*[7] studied Eu-implanted GaN and Eu *in situ* doped GaN grown by metal-organic chemical vapor deposition. They observed significant differences in the Eu^{3+} PL properties, including the number of emission lines associated with the $^5D_0 \rightarrow {}^7F_2$ transition. Based on optical spectroscopy and Rutherford backscattering studies, the authors concluded that the local symmetry of the Eu^{3+} ions has to be lower than C_{3V} symmetry.[7] Bang *et al.*[9] studied Eu-doped GaN prepared by gas-source molecular-beam epitaxy (MBE) and concluded, based on extended x-ray absorption fine-structure data, that Eu^{3+} occupies Ga sites with C_{3V} symmetry. It was also suggested that more than one local environment of Eu^{3+} ions may exist in the investigated GaN samples.

In this letter, we present PL results on GaN:Eu prepared by solid-source MBE, which provide spectroscopic evidence for the existence of different Eu^{3+} sites with distinct optical properties. Moreover, we report results of PL excitation (PLE) studies that identify the position of higher intra-4*f* Eu^{3+} energy levels as well as the existence of a broad defect band close to the conduction-band edge. This Eu-related defect level seems to play an important role in the efficient carrier-mediated excitation of Eu^{3+} ions in GaN.

The investigated GaN:Eu sample was prepared by solid-source MBE using a Riber MBE-32 system on a *p*-Si (111) substrate.[4] Solid sources were used to supply the Ga (7N purity) and Eu (3N purity) fluxes. A rf plasma source was used to generate atomic nitrogen. For the nitrogen plasma a rf power of 400 W and a N_2 flow rate of 1.5 sccm were employed. The Ga cell temperature ranged from 870 to 890 °C. A GaN buffer layer was first deposited for 10 min at a substrate temperature of 600 °C. For the main growth, the substrate temperature was ramped to 800 °C. The Eu cell temperature was 400 °C, resulting in an estimated Eu concentration of $\sim 10^{20}$–$10^{21}/\text{cm}^3$ (<2 at. %).

PL measurements were performed with an argon ion laser for above-gap (336.3–363.8 nm) and below-gap excitation (457.9 nm), respectively. For temperature-dependent PL studies the sample was mounted on the cold-finger of a two-stage, closed-cycle helium refrigerator. The visible emission was dispersed in a 1-m monochromator and detected with a thermoelectrically cooled photomulitiplier tube (PMT). PL lifetime measurements were performed with a third harmonic output of a pulsed Nd:YAG laser for above-gap excitation (355 nm). Below-gap excitation (~ 460 nm) was achieved using the output of an optical parametric oscillator (OPO)

a)Electronic mail: uwe.hommerich@hamptonu.edu

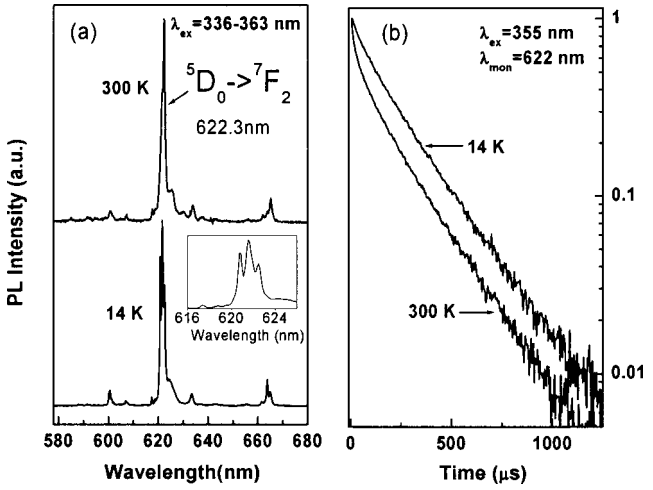

FIG. 1. (a) PL spectra of GaN:Eu under above-gap excitation (336–363 nm) at 14 and 300 K. (b) PL decay transients under above-gap excitation (355 nm) at 14 and 300 K. The inset in (a) shows the high-resolution spectrum in the region of the red Eu^{3+} line at 622.4 nm.

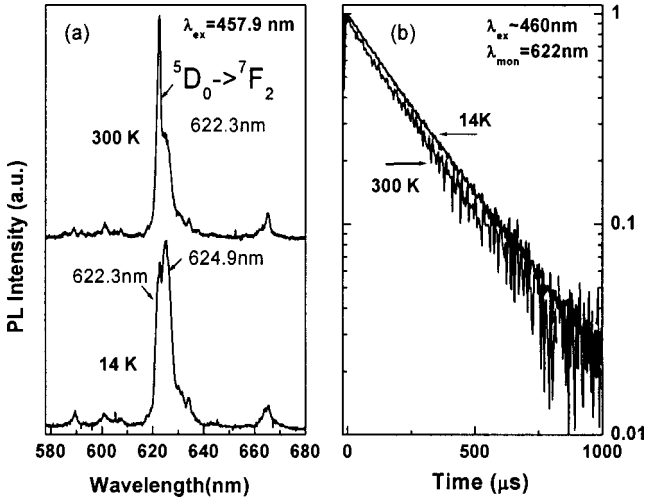

FIG. 2. (a) PL spectra of GaN:Eu under below-gap excitation (457.9 nm) at 14 and 300 K. (b) PL decay transients under below-gap excitation (460 nm) at 14 and 300 K.

system. The PL decay signals were detected by a PMT and averaged using a digitizing oscilloscope. The UV and visible output of a narrow-band ($\Delta\lambda \sim 0.1\ cm^{-1}$) OPO system were employed for PLE studies. The PLE spectrum was normalized to the pump energy of the excitation source.

High-resolution ($\Delta\lambda \sim 0.1$ nm) PL spectra of GaN:Eu at low (14 K) and room temperature under above-gap excitation are shown in Fig. 1(a). Characteristic intra-$4f$ Eu^{3+} emission lines were observed in the visible spectral region and were assigned in accordance with previous reports of Eu^{3+} ions in solid hosts.[14,15] The strongest Eu^{3+} emission line peaked at 622.3 nm and was attributed to the transition $^5D_0 \rightarrow {}^7F_2$. The full width half maximum (FWHM) linewidth of the 622.3 nm emission was determined to be ~ 1.6 nm at 300 K. This linewidth is less than half of the value reported by Li *et al.*[10] for GaN:Eu prepared by gas-source MBE on sapphire substrate, which indicates that the investigated sample is of higher crystalline quality and good uniformity. The inset in Fig. 1 shows that at 14 K, the red emission line splits into three main lines located at 620.8, 621.6, and 622.5 nm, and several weaker lines at shorter and longer wavelengths. For Eu^{3+} ions in C_{3V} site symmetry only three crystal-field levels are predicted for the $^5D_0 \rightarrow {}^7F_2$ transition.[15] The observation of more than three lines therefore suggests a local site symmetry lower than C_{3V}. An unambiguous assignment of the observed emission lines and Eu^{3+} site symmetry, however, is not possible because of the existence of different Eu^{3+} sites in GaN as will be discussed in the following. Moreover, it is possible that some emission lines arise from electron-phonon interactions and/or other impurities.[15]

The PL decay transients under-above gap excitation monitored at ~ 622 nm at 14 and 300 K are shown in Fig. 1(b). It can be noticed that the decay transients are slightly nonexponential with a fast initial decay component followed by a longer decaying component. Fitting the room-temperature transient to a double-exponential decay (inset equation) revealed that the fast decay component was $\sim 30\ \mu$s and the slow decay component had a value of $\sim 240\ \mu$s. Li *et al.* previously reported that GaN:Eu samples with Eu concentrations up to ~ 2.2 at. % do not show PL concentration quenching.[10] Therefore, energy transfer processes resulting in nonexponential decay behavior should be negligible in the investigated sample. Nonexponential decay transients have been observed previously for other RE-doped semiconductors (e.g., GaN:Er,[16,17] AlN:Er,[18] GaAs:Er,[19] Si:Er[20]) and were attributed to the existence of different Er^{3+} sites with distinct decay channels.

Direct evidence for the existence of different Eu^{3+} sites was obtained from PL measurements using below-gap excitation. Near resonant intra-$4f$ Eu^{3+} excitation was carried out using the 457.9-nm output of an argon-ion laser. The spectral resolution in these measurements was only ~ 0.8 nm because of the weaker signal strength compared to above-gap excitation. The low-temperature PL spectrum revealed significant spectral differences compared to above-gap excitation [Fig. 2(a)]. It can be noticed that the shoulder located at ~ 624.9 nm has gained significant intensity relative to the main line at 622.3 nm originating from the $^5D_0 \rightarrow {}^7F_2$ transition. Moreover, the Eu^{3+} decay transients at 14 and 300 K were found to be single exponential and nearly independent of temperature [Fig. 2(b)]. The PL decay time was determined to be $\sim 240\ \mu$s, which matched the slow-decaying component identified in the above-gap transients shown in Fig. 1(b). The data indicate that under below-gap excitation only a subset of the Eu^{3+} ions are selectively excited.

In Fig. 3 are shown the integrated PL intensity and lifetime of the red Eu^{3+} emission. Using above-gap excitation, the integrated PL was quenched by $\sim 90\%$ as the temperature increased from 14 to 300 K. The average PL lifetime (defined as the area under the decay transients), decreased only slightly ($\sim 10\%$) for the same temperature range indicating that nonradiative decay processes only weakly affect the Eu^{3+} PL. Therefore, the strong Eu^{3+} PL quenching under above-gap excitation is attributed to the temperature dependence of the carrier-mediated energy transfer process between the Eu^{3+} ions and the GaN host. Using below-gap pumping, the integrated Eu^{3+} PL intensity decreased by only a factor of 2 between 14 and 300 K, and the PL lifetime was nearly constant. Therefore, the weak Eu^{3+} PL quenching

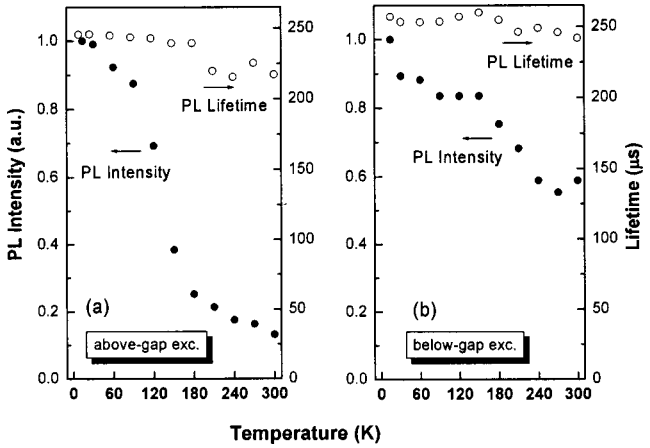

FIG. 3. Temperature dependence of the integrated PL intensity (solid circles) and PL lifetime (open circles) of GaN:Eu under (a) above-gap and (b) below-gap excitation.

with below-gap excitation is due to a slight change in the excitation efficiency.[21]

More information on the Eu^{3+} excitation and de-excitation properties was derived from PLE measurements depicted in Fig. 4. The PLE spectrum allows the identification of several intra-$4f$ Eu^{3+} absorption lines located at ~412 nm ($^7F_0 \rightarrow {}^5D_3$), ~471.2 nm ($^7F_0 \rightarrow {}^5D_2$), ~533.7 nm ($^7F_0 \rightarrow {}^5D_1$), ~543.5 nm ($^7F_1 \rightarrow {}^5D_1$), and ~590 nm ($^7F_1 \rightarrow {}^5D_0$). A broad excitation band (FWHM~21 nm) was centered at ~400 nm (3.1 eV), which overlapped the higher-lying Eu^{3+} transition $^7F_0 \rightarrow {}^5D_3$. This band also overlaps the transition $^7F_0 \rightarrow {}^5L_6$.[14] Based on Fourier transform infrared measurements, Li *et al.*[10] recently reported a Eu-related defect level at 0.37 eV below the conduction band of GaN. Such a band closely matches the observed broad PLE band identified in Fig. 4. The PLE results for GaN:Eu suggest that the broad-defect level provides an efficient pathway for the carrier-mediated energy transfer between Eu^{3+} ions and the GaN host. It is interesting to note that a defect level

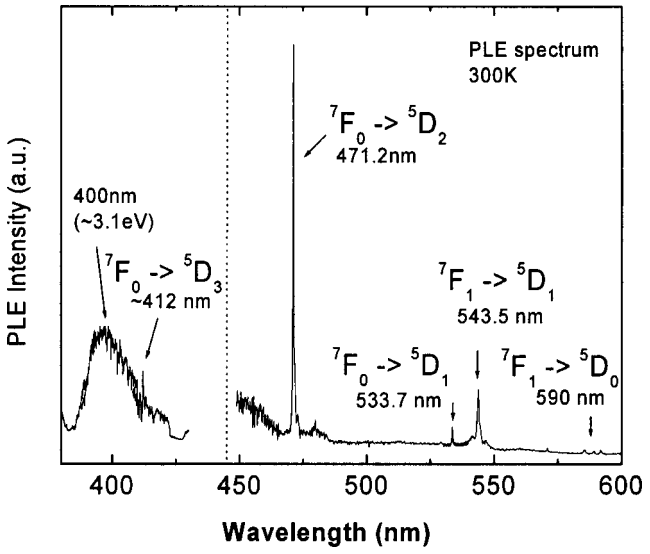

FIG. 4. PLE spectrum at 300 K of GaN:Eu monitored at 622.3 nm. The dotted line indicates a break in the relative PLE signal because of a change in the OPO excitation source.

~400 nm was also observed in the PLE spectra of Er-implanted GaN.[17] Previously, RE-related trap levels have been proposed as a means to explain the excitation of intra-$4f$ transitions of RE ions in other III–V semiconductors, e.g., InP:Yb[12] and GaAs:Er.[13]

In summary, we have obtained spectroscopic results of the optical properties of Eu^{3+} ions in GaN:Eu prepared by solid-source MBE. Wavelength-dependent PL studies revealed the existence of different Eu^{3+} centers with distinct optical properties. PLE measurements have provided evidence for a defect-related trap level that may be involved in the energy transfer between the GaN host and the Eu^{3+} ions. It seems likely that the carrier-mediated excitation of RE ions in III-nitrides can be optimized through careful manipulation of the RE-related defect levels and higher lying intra-$4f$ RE transitions. This manipulation could possibly be achieved through band-gap engineering of the host or through co-doping with sensitizer ions. Further comparative PLE studies of other RE-doped III-nitrides are currently in progress to support the defect-mediated excitation model.

The authors from H.U. acknowledge financial support by ARO grant DAAD19-02-1-0316 and AFOSR Instrumentation grant F49620-01-1-0528. The work at U.C. was supported by ARO grant DAAD19-99-1-0348.

[1] A. J. Steckl and J. M. Zavada, MRS Bull. **24**, 33 (1999).
[2] *Rare Earth Doped Semiconductors III*, Proceedings of E-MRS Symposium Spring 2000, edited by J. Zavada, T. Gregorkiewicz, and A. J. Steckl, [Mater. Sci. Eng., B **81** (2001) entire volume].
[3] A. J. Steckl, J. C. Heikenfeld, D. S. Lee, M. J. Garter, C. C. Baker, Y. Wang, and R. Jones, IEEE J. Sel. Top. Quantum Electron. **8**, 749 (2002).
[4] J. Heikenfeld, M. Garter, D. S. Lee, R. Birkhahn, and A. J. Steckl, Appl. Phys. Lett. **75**, 1189 (1999).
[5] S. Morishima, T. Maruyama, M. Tanaka, Y. Masumoto, and K. Akimoto, Phys. Status Solidi A **176**, 113 (1999).
[6] H. J. Lozykowski, W. M. Jadwisienczak, J. Han, and I. G. Brown, Appl. Phys. Lett. **77**, 767 (2000).
[7] T. Monteiro, C. Boemare, M. J. Soares, R. A. Sa Ferreira, L. D. Carlos, K. Lorenz, R. Vianden, and E. Alves, Physica B **308–310**, 22 (2001).
[8] M. Overberg, K. N. Lee, C. R. Abernathy, S. J. Pearton, W. S. Hobson, R. G. Wilson, and J. M. Zavada, Mater. Sci. Eng., B **81**, 150 (2001).
[9] H. Bang, S. Morishima, Z. Li, K. Akimoto, M. Nomura, and E. Yagi, J. Cryst. Growth **237–239**, 1027 (2002).
[10] Z. Li, H. Bang, G. Piao, J. Sawahata, and K. Akimoto, J. Cryst. Growth **240**, 382 (2002).
[11] E. E. Nyein, U. Hömmerich, J. Heikenfeld, D. S. Lee, A. J. Steckl, and J. M. Zavada, *OSA Technical Digest Vol. 73, Postconference Edition* (Optical Society of America, Washington, DC, 2002), p. 654.
[12] A. Taguchi and K. Takahei, J. Appl. Phys. **79**, 3261 (1996).
[13] K. Takahei, A. Taguchi, and R. A. Hogg, J. Appl. Phys. **82**, 3997 (1997).
[14] M. Dejneka, E. Snitzer, and R. E. Riman, J. Lumin. **65**, 227 (1995).
[15] A. A. Kaminskii, *Laser Crystals*, 2nd ed., Springer Series in Optical Sciences Vol. 14 (Springer, New York, 1990), p. 120.
[16] U. Hömmerich, J. T. Seo, C. R. Abernathy, A. J. Steckl, and J. M. Zavada, Mater. Sci. Eng., B **81**, 116 (2001).
[17] S. Kim, S. J. Rhee, X. Li, J. J. Coleman, S. G. Bishop, and P. B. Klein, J. Electron. Mater. **27**, 246 (1998).
[18] X. Wu, U. Hömmerich, J. D. Mackenzie, C. R. Abernathy, S. J. Pearton, R. G. Wilson, R. N. Schwartz, and J. M. Zavada, Appl. Phys. Lett. **70**, 2126 (1997).
[19] T. Benyattou, D. Seghier, G. Guillot, R. Moncorge, P. Galtier, and M. N. Charasse, Appl. Phys. Lett. **58**, 2132 (1991).
[20] F. Priolo, G. Franzo, S. Coffa, A. Polman, S. Libertino, R. Barklie, and D. Carey, J. Appl. Phys. **78**, 3874 (1995).
[21] J. T. Seo, U. Hömmerich, D. S. Lee, J. Heikenfeld, A. J. Steckl, and J. M. Zavada, J. Alloys Compd. **342**, 62 (2002).

Photoluminescence properties of *in situ* Tm-doped $Al_xGa_{1-x}N$

U. Hömmerich[a] and Ei Ei Nyein
Department of Physics, Hampton University, Hampton, Virginia 23668

D. S. Lee and A. J. Steckl
University of Cincinnati, Nanoelectronics Laboratory, Cincinnati, Ohio 45221

J. M. Zavada
US Army Research Office, Durham, North Carolina 27709

(Received 8 August 2003; accepted 10 October 2003)

We report on the photoluminescence (PL) properties of *in situ* Tm-doped $Al_xGa_{1-x}N$ films ($0 \leqslant x \leqslant 1$) grown by solid-source molecular-beam epitaxy. It was found that the blue PL properties of $Al_xGa_{1-x}N$:Tm greatly change as a function of Al content. Under above-gap pumping, GaN:Tm exhibited a weak blue emission at ~478 nm from the $^1G_4 \rightarrow {}^3H_6$ transition of Tm^{3+}. Upon increasing Al content, an enhancement of the blue PL at 478 nm was observed. In addition, an intense blue PL line appeared at ~465 nm, which is assigned to the $^1D_2 \rightarrow {}^3F_4$ transition of Tm^{3+}. The overall blue PL intensity reached a maximum for $x=0.62$, with the 465 nm line dominating the visible PL spectrum. Under below-gap pumping, AlN:Tm also exhibited intense blue PL at 465 and 478 nm, as well as several other PL lines ranging from the ultraviolet to near-infrared. The Tm^{3+} PL from AlN:Tm was most likely excited through defect-related complexes in the AlN host. © *2003 American Institute of Physics.* [DOI: 10.1063/1.1631742]

Light emission from rare-earth (RE)-doped III-N semiconductors is of significant current interest for applications in electroluminescence (EL) devices.[1–4] Previous work on visible emission from RE-doped III-Ns was mainly focused on RE-doped GaN.[1–3] Photoluminescence (PL) and cathodoluminescence (CL) data have been reported from nearly all lanthanide ions doped into GaN.[1–3] Visible EL devices based on RE-doped GaN, however, have only been demonstrated from GaN:Eu (red),[1,5,6] GaN:Er (green),[7] and GaN:Tm (blue).[8] One of the main challenges in using RE-doped GaN for full-color display applications is obtaining efficient blue emission. While dominant blue emission has been reported from GaN:Tm EL devices,[8,9] the overall device efficiency was significantly lower than results obtained for GaN:Eu (red) and GaN:Er (green).[2] For RE-doped AlN, red emission has also been reported from Eu, and green emission from Er- and Tb-doped amorphous and crystalline films.[10–12] Recently, blue CL was reported from Tm-impanted AlN[13] and efficient blue EL was demonstrated from *in situ* Tm-doped AlGaN films.[14]

In this letter, we report on the PL properties of $Al_xGa_{1-x}N$:Tm films under above- and below-gap pumping. Tm-doped $Al_xGa_{1-x}N$ films with $x=0$ (GaN), 0.16, 0.29, 0.39, 0.62, 0.81, and 1 (AlN) were grown by solid-source molecular-beam epitaxy on *p*-type Si (111) substrates. Elemental Al, Ga, and RE sources were used in conjunction with a rf-plasma source supplying atomic nitrogen. The Tm cell temperature was fixed at 600 °C, leading to a Tm concentration between ~0.2 and ~0.5 at. %. The $Al_xGa_{1-x}N$:Tm films were grown for 1 h at 550 °C and a growth rate of ~0.5 μm/h. Adjusting the Al cell temperature during growth controlled the Al content in the films. The total flux of Ga and Al was kept constant. The PL was excited using the UV output (250 nm, 10 ns pulses, 10 Hz repetition rate) of an optical parametric oscillator (OPO) system. For low-temperature PL measurements, the samples were mounted on the cold finger of a closed-cycle helium refrigerator. Visible PL spectra were recorded using a 0.5 m monochromator equipped with a photomultiplier tube for light detection. The signal was processed using a boxcar averager, and PL lifetime transients were recorded using a digitizing oscilloscope.

Figure 1 shows an overview of the normalized PL spectra of Tm-doped $Al_xGa_{1-x}N$ with $x=0$, 0.16, 0.21, 0.39, 0.62, and 0.81. The calculated bandgap energies using Vegard's law and a bowing parameter of $b=1$ are 3.39 eV (GaN), 3.71, 3.82, 4.26, 4.91, and 5.56 eV, respectively.[15] The PL was excited using the 250 nm (~4.96 eV) output of an OPO system, which corresponds to above-gap pumping for $Al_xGa_{1-x}N$ samples with $x \leqslant 0.62$. Similar to previous reports,[8,9] the visible PL from GaN:Tm is characterized by a broad band extending from ~400 to 600 nm and near-band-edge emission at ~367 nm. A weak blue PL line located at ~478 nm from the $^1G_4 \rightarrow {}^3H_6$ transition of Tm^{3+} is hardly observable. The infrared PL at ~803 nm is tentatively assigned to the intra-4*f* transition $^3H_4 \rightarrow {}^3H_6$ of Tm^{3+} ions.[9] Changing from GaN:Tm to $Al_xGa_{1-x}N$:Tm led to pronounced changes in the PL properties. Upon increasing Al content, the 478 nm PL line gained in intensity and was clearly observed. The broadband emission was also sharply reduced. The strongest emission from the $^1G_4 \rightarrow {}^3H_6$ transition at 478 nm was obtained for $x=0.39$. Interestingly, two other PL lines were observed: a weaker line at ~370 nm and a dominant blue line at ~465 nm. The PL intensity of the 465 nm line was several times larger compared to the 478 nm PL. The overall strongest blue PL intensity was measured

[a]Electronic mail: uwe.hommerich@hamptonu.edu

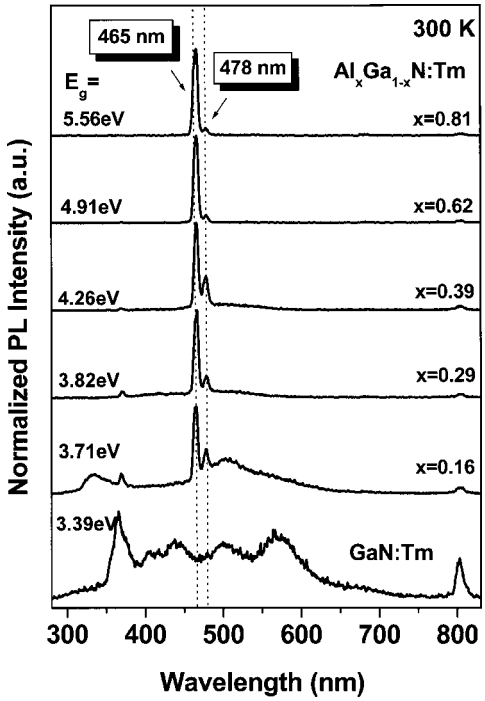

FIG. 1. Room-temperature PL spectra of $Al_xGa_{1-x}N$:Tm excited at 250 nm. The dotted lines indicate the position of the blue PL arising from the transitions $^1G_4 \rightarrow {}^3H_6$ (~478 nm) and $^1D_2 \rightarrow {}^3F_4$ (~465 nm). The calculated bandgap energies (E_g) are also indicated in the figure.

from $Al_{0.62}Ga_{0.38}N$:Tm with the 465 nm line being roughly ten times more intense than the 478 nm line.

The observation of new PL lines in $Al_xGa_{1-x}N$:Tm can be explained by the change in bandgap energy of the host. Tm^{3+} has higher excited states above the $^1G_4$ level, which are located at ~3.4 eV ($^1D_2$) and ~4.2 eV ($^1I_6/{}^3P_0$).[16,17] The energy of the $^1D_2$ level is very similar to the bandgap energy of GaN (see Fig. 3). Therefore, no emission from the $^1D_2$ level is observed from GaN:Tm. Upon increasing the bandgap energy of $Al_xGa_{1-x}N$, the D_2 level moves within the bandgap of the host, which results in the observation of PL lines at 370 and 465 nm. Based on the comparison to existing literature,[16,17] the 370 and 465 nm lines are assigned to the $^1D_2 \rightarrow {}^3H_6$ and $^1D_2 \rightarrow {}^3F_4$ transitions of Tm^{3+}.

Figure 1 also indicates that the excitation efficiency of the $^1G_4$ level of Tm^{3+} is enhanced in $Al_xGa_{1-x}N$:Tm samples compared to GaN:Tm. As mentioned earlier, hardly any blue Tm^{3+} PL was observed in GaN:Tm. A similar poor above-gap pumping efficiency was reported for Tb^{3+} ions in GaN:Tb.[18] The weak PL excitation efficiency was explained using a defect-related energy transfer model as proposed by Takahei *et al.* for RE-doped semiconductors.[19] In this model, RE doping of a semiconductor leads to the formation of RE-related levels in the bandgap of the host. These levels can trap free carriers, which subsequently recombine and transfer their energy to intra-4f RE transitions. Recent studies have identified RE-related traps for GaN:Eu,[19,20] GaN:Tb,[19] and GaN:Er[21] at ~0.3–0.4 eV below the conduction band of GaN. The recombination energy of carriers trapped at the RE-related defects in GaN is then estimated to be ~3.0–3.1 eV, which energetically matches intra-4f transitions of Eu^{3+} and Er^{3+}, respectively.[16] On the other hand, Tb^{3+} ions do not exhibit intra-4f transitions in that energy range, preventing an efficient carrier-mediated excitation process in GaN:Tb. Assuming that Tm^{3+} also induces a defect-level in GaN, similar arguments for the weak above-gap excitation efficiency can be applied to GaN:Tm Within the defect-related energy transfer model, however, the excitation efficiency of the Tm^{3+} can be optimized by a modification of the bandgap energy. Upon increasing Al content, higher excited states of Tm^{3+} ($^1D_2/{}^1I_6/{}^3P_J$) move within the bandgap of $Al_xGa_{1-x}N$, which provide additional channels for the energy transfer between defect levels and Tm^{3+} ions. Future investigations are necessary to identify Tm-related defects in $Al_xGa_{1-x}N$:Tm to support the defect-related energy transfer model. In addition, it cannot be excluded that chemical effects related to the presence of Al change the Tm^{3+} incorporation and excitation mechanisms, similar to observations made for Er-doped AlGaAs.[22]

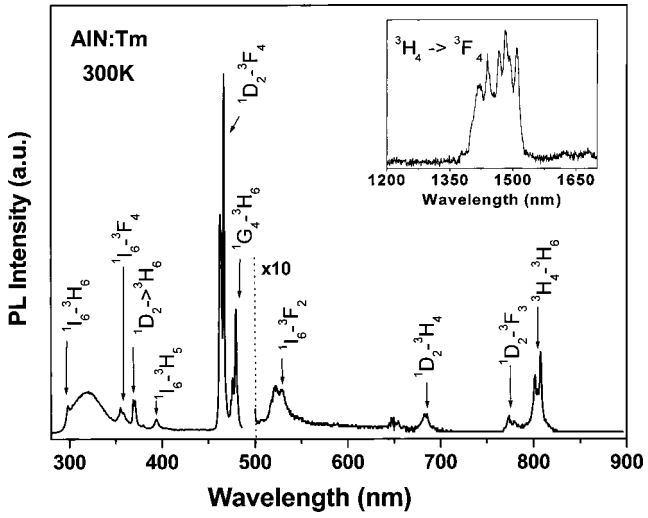

FIG. 2. High-resolution PL spectrum of AlN:Tm at room temperature. The PL was excited at 250 nm, which correspond to below-gap pumping. The assignment of the intra-4f transitions of Tm^{3+} is indicated in the figure. The inset shows the infrared PL spectrum around 1450 nm.

The high-resolution PL spectrum, with excitation at 250 nm, of AlN:Tm at room temperature is shown in Fig. 2. The PL was dominated by intense blue PL lines centered at ~465 and ~478 nm. The average lifetimes of the 465 and 478 nm lines were determined to be ~2 and ~33 μs, respectively. The lifetimes were nearly temperature independent, suggesting that nonradiative decay processes are small. The different

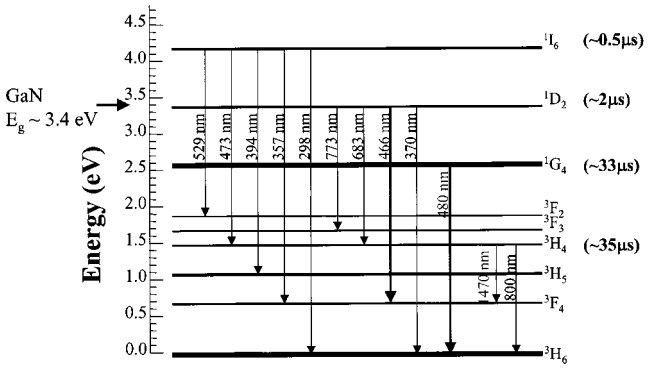

FIG. 3. Free-ion energy level diagram of Tm^{3+} ions and observed transitions in AlN:Tm. The bandgap of GaN is also indicated in the figure, along with PL lifetimes for several excited states of Tm^{3+}.

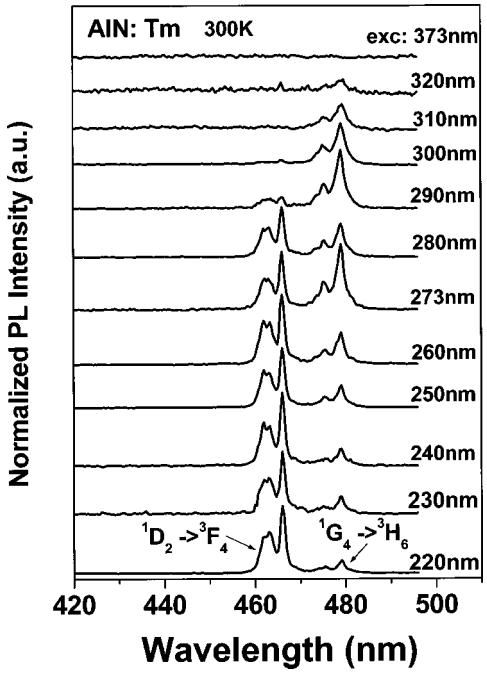

FIG. 4. Below-gap pumping of AlN:Tm using different excitation wavelengths in the UV region. The blue PL from Tm^{3+} can be excited of a wide range of wavelengths from ~320 down to 220 nm (lower wavelength limit of OPO laser system).

lifetimes also provide further support that the two blue PL lines arise from different transitions of Tm^{3+}, namely, $^1D_2 \rightarrow {}^3F_4$ (465 nm) and $^1G_4 \rightarrow {}^3H_6$ (478 nm). Besides the dominant blue PL, AlN:Tm exhibited several weaker PL lines ranging from the UV to the near-infrared spectral region. Emission at 1440 nm was also observed from AlN:Tm (inset of Fig. 2), which arises from the well-known Tm^{3+} transition $^3H_4 \rightarrow {}^3F_4$.[17] The identification of the remaining PL lines was facilitated by a careful analysis of PL lifetimes. It was found that the Tm^{3+} PL originates from four excited states of Tm^{3+}, namely, the $^1I_6$, $^1D_2$, $^1G_4$, and $^3H_4$ with room-temperature lifetimes of ~0.5, ~2, ~33, and ~35 μs, respectively (Fig. 3). Since the $^1G_4$ and $^3H_4$ states have similar PL lifetimes, the origin of the ~805 nm PL was clarified by pumping resonantly into the $^1G_4$ and $^3F_2$ excited state at ~478 and ~675 nm, respectively. Moreover, since the ~805 nm PL can be pumped resonantly in the $^3F_2$ excited state, it has to be due to the $^3H_4 \rightarrow {}^3H_6$ transition of Tm^{3+}. Based on the comparison to Tm^{3+}-doped insulating materials,[16,17] we tentatively located the $^1I_6$ level below the $^3P_0$ state. A final identification of the energy position of $^1I_6$ and $^3P_0$ levels, however, requires further investigations.

It is also interesting to note that the Tm^{3+} PL was efficiently excited below the bandgap of AlN using the 250 nm output from an OPO system. Since Tm^{3+} has no intra-4f transition absorption line close to 250 nm,[16] the excitation of Tm^{3+} ions in AlN must occur through defects in the AlN host. A similar below-gap excitation mechanism was observed for AlN:Er.[23] Excitation-wavelength-dependent studies showed that the Tm^{3+} PL can be excited over a wide wavelength range starting from ~320 down to 220 nm, as shown in Fig. 4. It can be seen that the ratio of emission from the $^1D_2$ (~465 nm) and $^1G_4$ (~478 nm) levels varied as a function of excitation wavelength. This result suggests the existence of different Tm^{3+} centers, which are selectively excited through different defects.

In summary, the PL properties of $Al_xGa_{1-x}N$:Tm were investigated. Under above-gap pumping, GaN:Tm exhibited only a weak blue emission from the $^1G_4 \rightarrow {}^3H_6$ transition of Tm^{3+}. A significant enhancement of the blue Tm^{3+} emission was observed from Tm-doped $Al_xGa_{1-x}N$ samples. Besides emission from the $^1G_4 \rightarrow {}^3H_6$ transition, a second blue emission line appeared around 465 nm, which was assigned to the $^1D_2 \rightarrow {}^3F_4$ transition of Tm^{3+}. The overall strongest blue PL emission was measured from $Al_xGa_{1-x}N$:Tm with $x=0.62$. Strong blue emission from the $^1D_2$ and $^1G_4$ levels of Tm^{3+} was also observed from AlN:Tm under below-gap excitation. The large sensitivity of the blue emission from Tm^{3+} on the Al content of $Al_xGa_{1-x}N$ indicates the possibility to optimize the RE excitation and emission properties through careful bandgap engineering of the host.

The authors from H. U. acknowledge financial support by ARO through grant DAAD19-02-1-0316. The work at U. C. was supported by ARO grant DAAD 19-99-1-0348.

[1] A. J. Steckl and J. M. Zavada, Mater. Res. Bull. **24**, 33 (1999).
[2] A. J. Steckl, J. C. Heikenfeld, D. S. Lee, M. J. Garter, C. C. Baker, Y. Wang, and R. Jones, IEEE J. Sel. Top. Quantum Electron. **8**, 749 (2002).
[3] Mater. Res. Soc. Symp. Proc. **422** (1996).
[4] *Proceedings of E-MRS Symposium Spring 2000*, edited by J. Zavada, T. Gregorkiewicz, and A. J. Steckl [Mater. Sci. Eng., B **81**, (2001)].
[5] S. Morishima, T. Maruyama, M. Tanaka, Y. Masumoto, and K. Akimoto, Phys. Status Solidi A **76**, 113 (1999).
[6] J. Heikenfeld, M. Garter, D. S. Lee, R. Birkhahn, and A. J. Steckl, Appl. Phys. Lett. **75**, 1189 (1999).
[7] A. Steckl and R. Birkhahn, Appl. Phys. Lett. **73**, 1700 (1998).
[8] A. J. Steckl, M. Garter, D. S. Lee, J. Heikenfeld, and R. Birkhahn, Appl. Phys. Lett. **75**, 2184 (1999).
[9] D. S. Lee and A. J. Steckl, Appl. Phys. Lett. **82**, 55 (2003).
[10] W. M. Jadwisienczak, H. J. Lozykowski, I. Berish, A. Bensaoula, and I. G. Brown, J. Appl. Phys. **89**, 4384 (2001).
[11] K. Gurumurugan, H. Chen, G. R. Harp, W. M. Jadwisienczak, and H. J. Lozykowski, Appl. Phys. Lett. **74**, 3008 (1999).
[12] V. I. Dimitrova, P. G. Van Patten, H. H. Richardson, and M. E. Kordesh, Appl. Phys. Lett. **77**, 478 (2000).
[13] U. Vetter, M. F. Reid, H. Hofsaas, C. Ronning, J. Zenneck, M. Dietrich, and ISOLDE Collaboration, MRS Proceedings **743**, L6.16.1 (2003).
[14] D. S. Lee and A. J. Steckl, Appl. Phys. Lett. **83**, 2094 (2003).
[15] D. G. Ebling, L. Kirste, K. W. Benz, N. Teofilov, K. Thonke, and R. Sauer, J. Cryst. Growth **227–228**, 453 (2001).
[16] G. H. Dieke, *Spectra and Energy Levels of Rare Earth Ions in Crystals* (Wiley, New York, 1968).
[17] M. D. Seltzer, J. B. Gruber, M. E. Hills, G. J. Quarles, and C. A. Morrison, J. Appl. Phys. **74**, 2821 (1993).
[18] H. Bang, S. Morishima, Z. Li, K. Akimoto, M. Nomura, and E. Yagi, Phys. Status Solidi B **228**, 319 (2001).
[19] K. Takahei, A. Taguchi, H. Nakagome, K. Uwai, and P. S. Whitney, J. Appl. Phys. **66**, 4941 (1989).
[20] E. E. Nyein, U. Hommerich, J. Heikenfeld, D. S. Lee, A. J. Steckl, and J. M. Zavada, Appl. Phys. Lett. **82**, 1655 (2003).
[21] S. Kim, S. J. Rhee, X. Li, J. J. Coleman, S. G. Bishop, and P. B. Klein, J. Electron. Mater. **27**, 246 (1998).
[22] T. Zhang, J. Sun, N. V. Edwards, D. E. Moxey, R. M. Kolbas, and P. J. Caldwell, Mater. Res. Soc. Symp. Proc. **301**, 257 (1993).
[23] X. Wu, U. Hömmerich, J. D. Mackenzie, C. R. Abernathy, S. J. Pearton, R. N. Schwartz, R. G. Wilson, and J. M. Zavada, Appl. Phys. Lett. **70**, 2126 (1997).

Materials Science and Engineering B105 (2003) 91–96

www.elsevier.com/locate/mseb

Photoluminescence studies of rare earth (Er, Eu, Tm) in situ doped GaN

U. Hömmerich [a,*], Ei Ei Nyein [a], D.S. Lee [b], J. Heikenfeld [b], A.J. Steckl [b], J.M. Zavada [c]

[a] *Department of Physics, Hampton University, Hampton, VA 23668, USA*
[b] *Nanoelectronics Laboratory, University of Cincinnati, Cincinnati, OH 45221, USA*
[c] *US Army Research Office, Durham, NC 27709, USA*

Abstract

The emission properties of rare earth (RE)-doped GaN are of significant current interest for applications in full color displays, white lighting technology, and optical communications. We are currently investigating the photoluminescence (PL) properties of RE (Er, Eu, Tm)-doped GaN thin-films prepared by solid-source molecular beam epitaxy. The most intense visible PL under above-gap excitation is observed from GaN:Eu (red: 622 nm) followed by GaN:Er (green: 537 nm, 558 nm), and then GaN:Tm (blue: 479 nm). In this paper, we present spectroscopic results on the Ga-flux dependence of the Er^{3+} PL properties from GaN:Er and we report on the identification of different Eu^{3+} centers in GaN:Eu through high-resolution PL excitation (PLE) studies. In addition, we observed an enhancement of the blue Tm^{3+} PL from AlGaN:Tm compared to GaN:Tm. Intense blue PL from Tm^{3+} ions was also obtained from AlN:Tm under below-gap pumping.

PACS: 78.40. Fy; 78.55.-m; 78.55.Et

Keywords: Rare earth; GaN; AlGaN; Luminescence

1. Introduction

Rare earth (RE)-doped III-nitrides have recently emerged as a new class of phosphor materials for thin- and thick-film electroluminescence devices [1–4]. Compared to previously studied RE-doped semiconductors with relatively small band-gap (<∼1.5 eV) like e.g. GaAs or Si [5], RE doping of wide band-gap semiconductors such as GaN, AlN, and SiC has led to the observation of intense RE emission at room temperature [6,7]. In addition, studies of GaN:Er and GaN:Eu have shown that RE^{3+} ions can be incorporated into GaN at concentrations as high as 1–2 at.% without significant emission concentration quenching [8,9]. Current research efforts on RE-doped nitrides are focused on the optimization of existing materials and EL devices [2,3,7], evaluation of different doping techniques and dopant/host combinations [4,7,10–12], as well as fundamental spectroscopic studies aimed towards a better understanding of the RE incorporation, excitation schemes, and emission efficiency [7,13–16].

In this paper, we present spectroscopic results of the PL properties of GaN:Er as a function of Ga-flux employed during molecular beam epitaxy (MBE) growth. As will be discussed in more detail, the Ga-flux during growth significantly impacts the Er^{3+} lattice location and the concentration of optically active Er^{3+} ions. High-resolution PL excitation (PLE) studies were carried out on GaN:Eu, which allowed the identification of $^5D_0 \leftrightarrow {}^7F_0$ transitions and associated Eu^{3+} centers. Finally, we report on initial PL studies of Tm-doped $Al_xGa_{1-x}N$ ($0 \leq x \leq 1$) and the enhancement of the blue Tm^{3+} emission with increasing Al content.

2. Experimental details

Rare earth (Er, Eu, Tm)-doped GaN and Tm-doped $Al_xGa_{1-x}N$ films with $x = 0.13$, 0.24, 0.29, 0.44, and 1 (AlN) were grown by solid-source MBE on p-type Si(1 1 1) substrates. Elemental Ga, Al, and RE sources were used in conjunction with a radio frequency (rf)-plasma source supplying atomic nitrogen. The RE concentration in the GaN and AlGaN films varied between ∼0.5 and ∼1 at.%. More details on the sample preparation were published previously [2,17].

* Corresponding author. Tel.: +1-757-727-5829; fax: +1-757-728-6910.
E-mail address: uwe.hommerich@hamptonu.edu (U. Hömmerich).

0921-5107/$ – see front matter © 2003 Elsevier B.V. All rights reserved.
doi:10.1016/j.mseb.2003.08.022

PL spectra were measured using either the UV argon laser lines (336–363 nm) or a visible argon laser line at 496.5 nm. PL excitation spectra were recorded using an Optical Parametric Oscillator system as the excitation source. For low-temperature PL measurements the samples were mounted on the cold-finger of a closed-cycle helium refrigerator. Infrared PL spectra were recorded using a 1 m monochromator equipped with a liquid-nitrogen cooled Ge detector. In visible PL studies a thermo-electric cooled photomultiplier tube was employed for detection. The signal was processed using lock-in techniques or using a boxcar averager. The obtained PL spectra were not corrected for the spectral response of the setup.

3. Results and discussion

3.1. Er-doped GaN

It was previously reported that the visible and infrared emission properties of Er^{3+} ions in GaN films are strongly dependent on the Ga-flux during growth [18]. Under above band-gap excitation the Er^{3+} PL emission reached its maximum under slightly N-rich growth conditions. On the contrary, the band-edge emission from the GaN host reached its maximum under Ga-rich growth. This observation lead to the conclusion that the Ga-flux strongly influences the carrier-mediated excitation efficiency of Er^{3+} ions [18]. In the following, more detailed spectroscopic study on the Ga-flux dependence of the Er^{3+} PL properties are presented. Er-doped GaN samples grown under Ga-fluxes with beam equivalent pressures ranging from 2.2×10^{-7} Torr ("N-rich") to 6.9×10^{-7} Torr ("Ga-rich") were investigated [18]. The stoichiometric growth condition as determined by film thickness saturation was ~4 to 5×10^{-7} Torr.

The visible and IR PL spectra under below band-gap excitation (496.5 nm) are shown in Fig. 1. This excitation wavelength overlaps an intra-4f Er^{3+} absorption line ($^4I_{15/2} \rightarrow {}^4F_{9/2}$) [19,20]. Similar to above-gap excitation [18], the Er^{3+} PL strongly varied with Ga-flux under resonant excitation and reached a maximum under slightly N-rich growth condition. Since both excitation schemes, carried-mediated and resonant intra-4f, exhibited the same Er^{3+} PL behavior it can be concluded that the carrier-mediated Er^{3+} excitation is only weakly affected by the Ga-flux during growth.

Fig. 2 shows the high-resolution 1.54 μm Er^{3+} PL spectra of GaN:Er samples grown under different Ga-fluxes. A significant decrease in the 1.54 μm PL linewidth can be noticed as well as the appearance of new spectral features with increasing Ga-flux. The spectral narrowing of the emission lines is consistent with the higher crystalline quality of GaN grown under Ga-rich conditions [18,21]. The observation of new spectral lines indicates that Er^{3+} ions are incorporated into different lattice locations depending on the Ga-flux.

More information on the optical activation of Er^{3+} in GaN can be drawn from power dependent PL studies under above-gap excitation (see Fig. 3). All investigated samples exhibited the onset of 1.54 μm PL saturation at relatively low pump intensities (<2 W/cm^2), consistent with a high excitation efficiency for above-gap pumping [16]. At the same time, it can be noticed that the Er^{3+} PL saturation level greatly varied for the different samples. It has been discussed in the literature before [16,22], that the Er^{3+} PL saturation level is determined by the product of concentration of optically active Er ions (N_{Er}) and radiative decay rate (w_{rad}). PL lifetime studies revealed that w_{rad} is approximately independent of Ga-flux. Therefore, the large difference in the PL saturation is attributed to a large difference in the concentration of optically active Er^{3+} ions. As can be derived from Fig. 3, the PL saturation level and hence N_{Er} is ~17 times larger for the sample grown under slightly N-rich con-

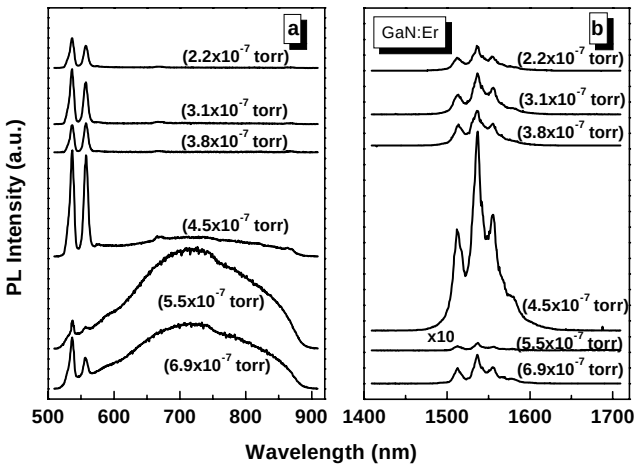

Fig. 1. Visible (a) and infrared (b) emission from Er-doped GaN as a function of Ga-flux under below-gap excitation (496.5 nm). For both cases, the Er^{3+} emission intensity reached its maximum under slightly N-rich flux near the stoichiometric growth condition (Ga-flux: $\sim 4.5 \times 10^{-7}$ Torr).

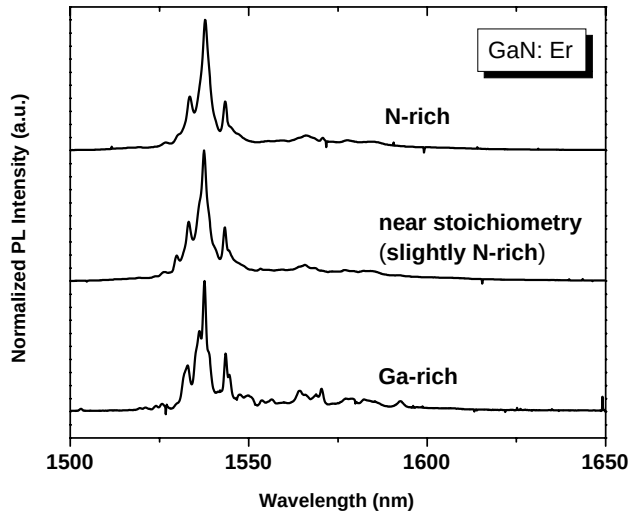

Fig. 2. High-resolution, infrared emission spectra at 15 K from Er-doped GaN grown under different Ga-fluxes. The emission was excited using below-gap excitation (496.5 nm).

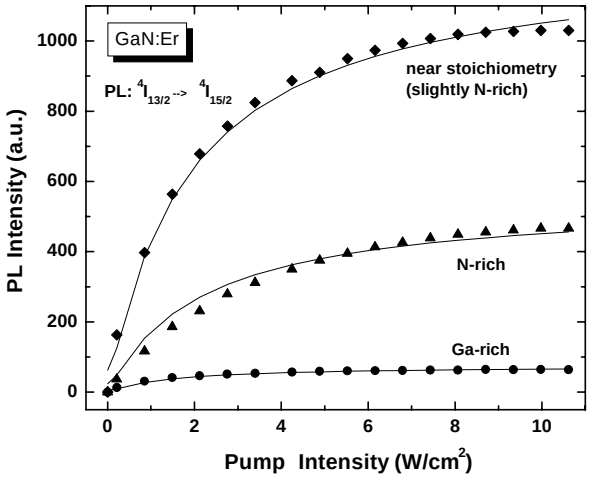

Fig. 3. Pump intensity dependence of the 1.54 μm PL from GaN:Er samples grown with different Ga-flux during growth. The emission was excited using above-gap excitation (336–363 nm). The solid lines are guides for the eye.

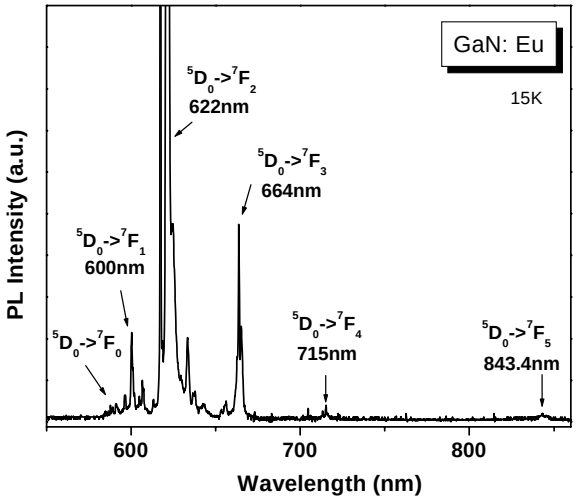

Fig. 4. Emission spectrum of GaN:Eu at 15 K under above-gap excitation. The main emission features arising from the $^5D_0$–^7F_J ($J = 0,1,2,3,4,5$) transitions are indicated in the graph. More details on the identification of the $^5D_0$–$^7F_0$ transitions are presented in Fig. 5.

ditions compared to that grown under Ga-rich conditions. In contrast, previous secondary ion mass spectroscopy (SIMS) studies have shown that the total Er concentration in the investigated GaN:Er films varied only by roughly a factor of two [18]. Therefore, the PL saturation result from Fig. 3 reveal that in GaN:Er grown under Ga-rich conditions only a small fraction (<10%) of the total Er concentration is optically active under above-gap pumping. Similar observations were reported for Er-doped crystalline and amorphous Si [23]. More comparative PL saturation studies employing a well-characterized Er^{3+} sample (e.g. Er-doped SiO_2) are required to determine the absolute concentration of optically active Er^{3+} ions in GaN:Er.

3.2. Eu-doped GaN

Eu-doped GaN is of great interest for display applications because of its bright red emission peaking around 622 nm [14,24–28]. Eu^{3+} is also known as a "spectroscopic probe" for the local environment of Eu^{3+} ions in solids, because the main emitting level is the non-degenerate $^5D_0$ state [20]. For example, observing the $^5D_0 \leftrightarrow {}^7F_0$ transition allows one to identify the number of emitting Eu^{3+} centers in a given host. Fig. 4 gives an overview of the low temperature emission of GaN:Eu. The main emission lines can be assigned to the transitions: $^5D_0 \rightarrow {}^7F_5$ (~843 nm), $^5D_0 \rightarrow {}^7F_4$ (~715 nm), $^5D_0 \rightarrow {}^7F_3$ (~664 nm), $^5D_0 \rightarrow {}^7F_2$ (~622 nm), and $^5D_0 \rightarrow {}^7F_1$ (~600 nm). The weak emission features at ~585 and ~590 nm are most likely due to $^5D_0 \rightarrow {}^7F_0$ transitions suggesting multiple Eu^{3+} centers in GaN [14,27,28].

In order to identify the $^5D_0 \leftrightarrow {}^7F_0$ transitions and associated Eu^{3+} centers more clearly, we have performed high-resolution PL excitation studies in the range from 560 to 595 nm. The spectral resolution in the PLE measurements was limited by the linewidth of the employed excitation source (~0.2 cm^{-1}) (Fig. 5).

At room temperature, four PLE peaks were observed at 571, 585.2, 588.8, and 591.7 nm. With decreasing temperature the peak at 591.7 nm reduced in intensity and was not observed at 15 K. Therefore, this line does not originate from the $^7F_0$ ground state, but is due to the thermal population of higher lying $^7F_1/{}^7F_2$ manifolds. The linewidth of all PLE peaks observed at room-temperature narrowed slightly with decreasing temperature and some fine structure was resolved. At low temperature (15 K) five PLE lines at 571, 585.8, 587.9, 588.9, and 589.4 nm were observed and tentatively assigned to $^7F_0 \rightarrow {}^5D_0$ transitions. The $^7F_0 \rightarrow {}^5D_0$ transition at ~571 nm is at an unusually low wavelength, but similar cases have been reported [29,30]. Therefore, we conclude that at least five different Eu^{3+} centers exist in GaN:Eu.

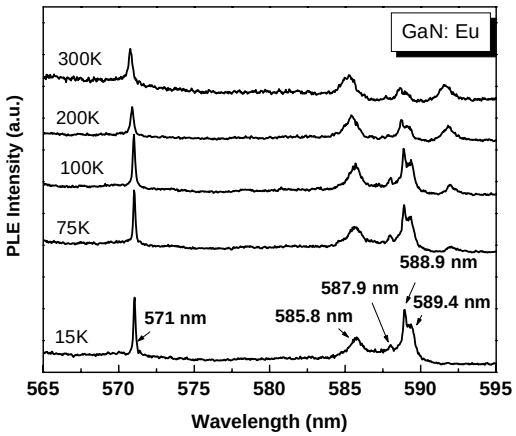

Fig. 5. High-resolution PLE spectrum of Eu-doped GaN at 15 K. The emission was monitored at ~623 nm. Absorption lines located at 571, 585.5, 587.9, 588.9, and 589.4 nm are tentatively assigned to the $^7F_0$–$^5D_0$ transitions.

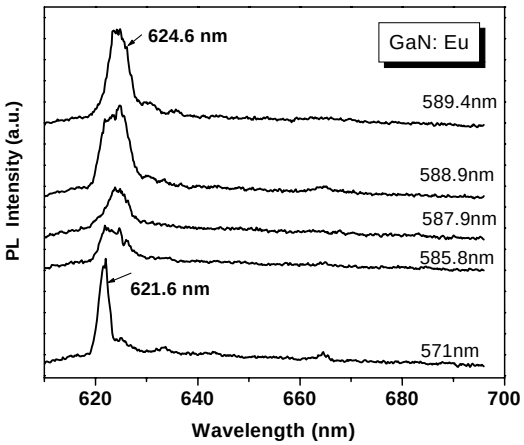

Fig. 6. Site-selective PL spectra at 15 K excited at 571, 585.5, 587.9, 588.9, and 589.4 nm. The Eu^{3+} center excited at 571 nm is distinct from the other Eu^{3+} centers and dominates under above-gap excitation.

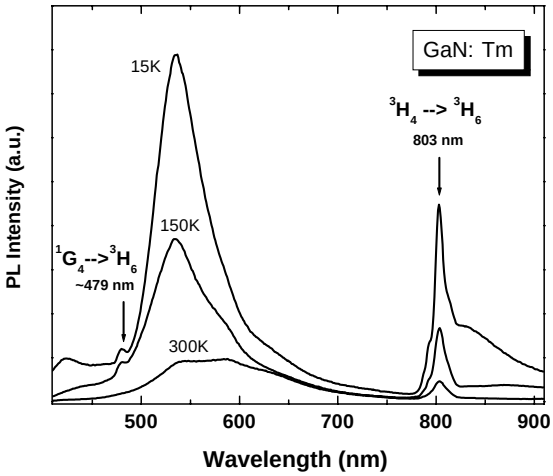

Fig. 7. PL spectra of Tm-doped GaN under above-gap excitation at 15, 150, and 300 K. The shoulder at 479 nm indicates blue emission from the $^1G_4 \rightarrow {}^3H_6$ intra-4f transition of Tm^{3+}.

More support for the identification of the different Eu^{3+} centers was obtained from site-selective PL measurements. Pumping resonantly into each of the PLE line revealed different Eu^{3+} emission spectra and lifetimes as shown in Fig. 6. The spectral differences are especially pronounced for the Eu^{3+} center excited at 571 nm. This Eu^{3+} center exhibited a relatively narrow $^5D_0 \rightarrow {}^7F_2$ PL at ~622 nm with a nearly exponential lifetime of ~235 μs. The $^5D_0 \rightarrow {}^7F_2$ PL spectra of the other Eu^{3+} centers are broader and shifted to longer wavelength (~624 nm). In addition, the PL decay transients of these Eu^{3+} centers are non-exponential with average lifetimes of less than 200 μs. The smaller linewidth of the 571 nm Eu^{3+} center indicates less inhomogeneous broadening compared to the other Eu^{3+} centers. It can be speculated that the 571 nm center is associated with Eu^{3+} ions in substitutional Ga^{3+} lattice positions, whereas the other Eu^{3+} centers are due to Eu^{3+} ions incorporated into interstitial sites with close vicinity to other defects and impurities. Interestingly, the PL spectrum excited at 571 nm is very similar to PL spectra obtained under above-gap pumping, which shows that this Eu^{3+} center dominates under carrier-mediated excitation. More site-selective PL and PLE studies of the different Eu^{3+} centers in GaN are in progress.

3.3. *Tm-doped $Al_xGa_{1-x}N$ ($0 \leq x \leq 1$)*

PL spectra of Tm-doped GaN under above-gap excitation at 15, 150, and 300 K are shown in Fig. 7. The emission is dominated by a broad band centered at ~530 nm, which extends from roughly 450 to 750 nm and resembles the well-known yellow band emission from GaN [31,32]. An infrared emission line at ~803 nm can be assigned to the intra-4f transition $^3H_4 \rightarrow {}^3H_6$ of Tm^{3+} ions [33]. A weak shoulder at ~479 nm indicates the blue emission line from the $^1G_4 \rightarrow {}^3H_6$ transition of Tm^{3+}. The PL intensity of 479 nm line increases slightly when cooling the sample down to 15 K. Compared to the visible PL from GaN:Er and GaN:Eu, the blue emission from GaN:Tm is orders of magnitude weaker under above-gap pumping, which indicates that Tm^{3+} ions are not efficiently excited through carrier recombination processes.

An energy transfer model based on a RE-related trap level was proposed by Takahei et al. for InP:Yb and later extended to other RE-doped semiconductors [34,35]. In this model, RE doping of a semiconductor leads to the formation of a RE related level in the band-gap of the host. This level can trap photo-excited free carriers, which subsequently recombine and transfer their energy to intra-4f RE transitions. Our recent PL excitation measurements of GaN:Eu provided experimental evidence for an Eu trap-level at ~0.3 eV below the conduction band of GaN [27]. A similar level was reported by Li et al. using Fourier transform infrared (FTIR) measurements [9] and by Vantomme et al. using deep level transient spectroscopy (DLTS) [36]. An Er related trap-level at ~0.3 eV was also reported for GaN:Er [37]. The recombination energy of carriers trapped at the Eu/Er related traps in GaN is then estimated to be ~3.1 eV, which energetically matches intra-4f transitions of Eu^{3+} and Er^{3+}, respectively [19]. Therefore, the carrier-mediated energy transfer to Er^{3+} and Eu^{3+} seems to occur with high efficiency. On the contrary, the energy level structure of Tm^{3+} does not exhibit an energy level at ~3.1 eV. Consequently, a carrier-mediated energy transfer process to Tm^{3+} ions is less likely to occur in GaN:Tm. A similar explanation was recently proposed for the poor above-gap excitation efficiency of Tb^{3+} ions in GaN:Tb [9].

In an effort to optimize the carrier-mediated excitation of Tm^{3+} ions in III-nitrides, we are currently exploring the energy transfer process to Tm^{3+} as a function of band-gap energy. Fig. 8 shows preliminary emission spectra for Tm-doped $Al_xGa_{1-x}N$ with $x = 0$ (GaN), 0.13,0.24, 0.29, 0.44, and 1 (AlN). The corresponding band-gap energies are 3.4 eV (GaN), 3.64, 3.88, 3.99, 4.89, and 6.2 eV (AlN)

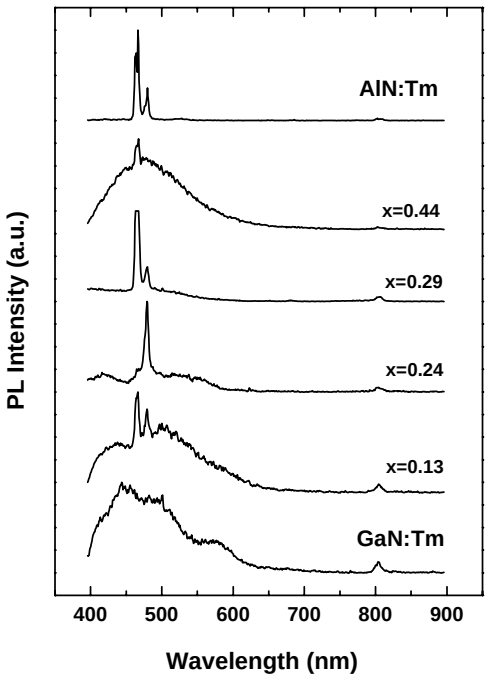

Fig. 8. PL spectra of Tm-doped $Al_xGa_{1-x}N$ with $x = 0$ (GaN), 0.13, 0.24, 0.29, 0.44, and 1 (AlN) under 250 nm excitation.

respectively. The emission was excited at 250 nm, which corresponds to above-gap pumping for all investigated AlGaN samples, but results in below-gap excitation for AlN:Tm. As discussed before, hardly any blue emission was observed from GaN:Tm (lowest trace in Fig. 8). With increasing Al content an enhancement of the 478 nm line from Tm^{3+} is observed. In addition, a new blue emission line appears at ~466 nm. Based on a comparison to existing literature [38], the 466 nm line is tentatively attributed to emission from the $^1D_2 \rightarrow {}^3F_4$ transition of Tm^{3+} ions. The overall blue emission from both lines at 466 and 479 nm reached a maximum for an Al content of $x = 0.29$, with the 466 nm line having the highest PL intensity. At higher Al content the total blue emission started to decrease and at $x = 0.44$ only weak blue emission at 466 nm was observed. On the contrary, below-gap pumping at 250 nm of AlN:Tm resulted into strong blue emission with intense lines at ~466 and 479 nm. For AlN:Tm, the blue emission is most likely excited through some broad defect level in the host.

Fig. 8 clearly demonstrates the sensitivity of the blue Tm^{3+} emission on the Al content and hence the band-gap of AlGaN. It cannot be excluded, however, that also chemical effects related to the presence of Al change the Tm^{3+} incorporation and excitation mechanisms, similar to observations made for Er-doped AlGaAs [39,40]. The initial spectroscopic data on $Al_xGa_{1-x}N$:Tm indicate that the excitation efficiency of the $^1G_4$ state of Tm^{3+} increases up to $x \sim 0.24$. In addition, the larger bandgap of AlGaN compared to GaN moves the $^1D_2$ level of Tm^{3+} within the band-gap of the host, which results in emission at 466 nm. A more detailed analysis of the emission properties of AlGaN:Tm and AlN:Tm is still in progress and will be discussed in a forthcoming paper.

4. Conclusions

Spectroscopic results on the PL properties of GaN:Er, GaN:Eu, GaN:Tm and AlGaN:Tm were presented. High-resolution PL and pump-power dependent PL studies of GaN:Er samples revealed that the Er^{3+} incorporation and the concentration of optically active Er ions is strongly dependent on the Ga-flux during MBE growth. Based on PL saturation experiments, we concluded that only a small fraction (<10%) of the total Er ions in GaN are optically active for samples grown under Ga-rich conditions. More PL saturation experiments are still in progress to determine the absolute concentration of optically active Er^{3+} ions in GaN:Er films. The low optical activation of Er^{3+} ions in GaN is similar to recent observations made for Er-doped Si/amorphous Si [23]. This issue needs to be further addressed in future investigations to explore the full potential of RE-doped GaN for device applications. High-resolution PL excitation studies were performed on GaN:Eu and allowed the identification of at least five Eu^{3+} centers. An absorption line at an unusually low wavelength of ~571 nm was also tentatively assigned to the $^5D_0 \leftrightarrow {}^7F_0$ transition. The Eu^{3+} center selectively excited through this 571 nm absorption line is distinct from the other Eu^{3+} centers and seems to dominate the above-gap pumped PL emission spectrum. GaN:Tm exhibited only a weak blue emission from the $^1G_4 \rightarrow {}^3H_6$ transition of Tm^{3+} ions. A significant enhancement of the blue Tm^{3+} emission was obtained under above-gap pumping of Tm-doped $Al_xGa_{1-x}N$ samples. Besides emission from the $^1G_4 \rightarrow {}^3H_6$ transition, a second blue emission line appeared around 466 nm for $x > 0.13$, which was assigned to the $^1D_2 \rightarrow {}^3F_4$ transition of Tm^{3+}. Strong blue emission from the $^1D_2$ and $^1G_4$ levels of Tm^{3+} was also observed from Tm-doped AlN under below-gap excitation. The large sensitivity of the blue emission from Tm^{3+} on the band-gap of AlGaN suggests the possibility to optimize the RE excitation and emission properties through careful band-gap engineering of the host.

Acknowledgements

The authors from H.U. acknowledge financial support by ARO through grant DAAD19-02-1-0316. The work at U.C. was supported by ARO grant DAAD19-99-1-0348. Helpful discussions with F. Pelle and F. Auzel are also acknowledged.

References

[1] A.J. Steckl, J.M. Zavada, MRS Bull. 24 (9) (1999) 33–38.
[2] A.J. Steckl, J.C. Heikenfeld, D.S. Lee, M.J. Garter, C.C. Baker, Y. Wang, R. Jones, IEEE J. Sel. Top. Quant. 8 (2002) 749.

[3] S. Morishima, T. Maruyama, M. Tanaka, Y. Masumoto, K. Akimoto, Phys. Stat. Sol. A 176 (1999) 113.
[4] V.I. Dimitrova, P.G. Van Patten, H.H. Richardson, M.E. Kordesh, Appl. Phys. Lett. 77 (2000) 478.
[5] Rare earth doped semiconductors. I, in: G.S. Pomerenke, P.B. Klein, D.W. Langer (Eds.), Proceedings of the Materials Research Society, Vol. 301, 1993.
[6] Rare earth doped semiconductors. II, in: S. Coffa, A. Polman, R.N. Schwartz, (Eds.), Proceedings of the Materials Research Society, Vol. 422, 1996.
[7] Rare earth doped semiconductors. III, in: J. Zavada, T. Gregorkiewicz, A.J. Steckl (Eds.), Proceedings of E-MRS Symposium Spring 2000, Mater. Sci. Eng. B 81 (2001).
[8] D.S. Lee, J. Heikenfeld, A.J. Steckl, U. Hömmerich, J.T. Seo, A. Braud, J.M. Zavada, Appl. Phys. Lett. 79 (2001) 719.
[9] Z. Li, H. Bang, G. Piao, J. Sawahata, K. Akimoto, J. Cryst. Growth 240 (2002) 382.
[10] J.T. Torvik, C.H. Qui, R.J. Feuerstein, J.I. Pankove, F. Namavar, J. Appl. Phys. 81 (1997) 6343.
[11] H.J. Lozykowski, W.M. Jadwisienczak, I.G. Brown, Appl. Phys. Lett. 74 (1999) 1129.
[12] E. Alves, M.F. da Silva, J.C. Soares, R. Vianden, J. Bartels, A. Kozanecki, Nucl. Instrum. Methods B 147 (1999) 383.
[13] S. Kim, S.J. Rhee, X. Li, J.J. Coleman, S.G. Bishop, P.B. Klein, J. Electron. Mater. 27 (1998) 246.
[14] T. Monteiro, C. Boemare, M.J. Soares, R.A. Sa Ferreira, L.D. Carlos, K. Lorenz, R. Vianden, E. Alves, Physica B 308–310 (2001) 22.
[15] U. Wahl, A. Vantomme, G. Langouche, J.P. Araujo, L. Peralta, J.G. Correia,. The ISOLDE collaboration J. Appl. Phys. 88 (2000) 1319.
[16] J.T. Seo, U. Hömmerich, D.S. Lee, J. Heikenfeld, A.J. Steckl, J.M. Zavada, J. Alloys Comp. 342 (2002) 62.
[17] A. Steckl, R. Birkhahn, Appl. Phys. Lett. 73 (1998) 1700.
[18] D.S. Lee, A.J. Steckl, Appl. Phys. Lett. 80 (2002) 728.
[19] G.H. Dieke, Spectra and Energy Levels of Rare Earth Ions in Crystals, Wiley, New York, 1968.
[20] B. Henderson, G.F. Imbusch, Optical Spectroscopy of Inorganic Solids, Clarendon Press, Oxford, UK, 1989.
[21] E. Calleja, M.A. Sanchez-Garcia, F.J. Sanchez, F. Calle, F.B. Naranjo, E. Munoz, U. Jahn, K. Ploog, Phys. Rev. B 62 (2000) 16826.
[22] F. Priolo, G. Franzo, S. Coffa, A. Carnera, Phys. Rev. B. 57 (1998) 4443.
[23] O.B. Gusev, M.S. Bresler, P.E. Pak, I.N. Yassievich, M. Forcales, N.Q. Vinh, T. Gregorkiewicz, Phys. Rev. B 64 (2001) 075302.
[24] J. Heikenfeld, M. Garter, D.S. Lee, R. Birkhahn, A.J. Steckl, Appl. Phys. Lett. 75 (1999) 1189.
[25] H.J. Lozykowski, W.M. Jadwisienczak, J. Han, I.G. Brown, Appl. Phys. Lett. 77 (2000) 767.
[26] M. Overberg, K.N. Lee, C.R. Abernathy, S.J. Pearton, W.S. Hobson, R.G. Wilson, J.M. Zavada, Mater. Sci. Eng. B 81 (2001) 150.
[27] E.E. Nyein, U. Hommerich, J. Heikenfeld, D.S. Lee, A.J. Steckl, J.M. Zavada, Appl. Phys. Lett. 82 (2003) 1655.
[28] H. Bang, S. Morishima, Z. Li, K. Akimoto, M. Nomura, E. Yagi, Phys. Stat. Sol. B 228 (2001) 319.
[29] R. Ternane, G. Panczer, M.Th. Cohen-Adad, C. Goutaudier, G. Boulon, N. Kbir-Ariguib, M. Trabesli-Ayedi, Opt. Mater. 16 (2001) 291.
[30] E. Antic-Fidancev, J. Alloys Comp. 300301 (2002) 2.
[31] T. Ogino, M. Aoki, Jpn. J. Appl. Phys. 19 (1980) 2395.
[32] S.J. Pearton, J.C. Zolper, R.J. Shul, F. Ren, J. Appl. Phys. 86 (1999) 1.
[33] D.S. Lee, A.J. Steckl, Appl. Phys. Lett. 82 (2003) 55.
[34] K. Takahei, A. Taguchi, H. Nakagome, K. Uwai, P.S. Whitney, J. Appl. Phys. 66 (1989) 4941.
[35] A. Taguchi, K. Takahei, J. Appl. Phys. 79 (1996) 4330.
[36] A. Vantomme, B. Pipeleers, V. Matias, E. Alves, K. Lorenz, R.W. Martin, S. Dalmasso, K.P. O'Donnell, A. Braud, J.L. Doualan, European Materials Society Spring Meeting 2003, Strasbourg, France, paper J-VI.1.
[37] S. Kim, S.J. Rhee, X. Li, J.J. Coleman, S.G. Bishop, P.B. Klein, J. Electron. Mater. 27 (1998) 246.
[38] J.B. Gruber, A.O. Wright, M.D. Selter, B. Zandi, L.D. Merkle, J.A. Hutchinson, C.A. Morrison, T.H. Allik, B.H.T. Chai, J. Appl. Phys. 81 (1997) 6585.
[39] T. Zhang, J. Sun, N.V. Edwards, D.E. Moxey, R.M. Kolbas, P.J. Caldwell, Mater. Res. Soc. Symp. Proc. 301 (1993) 257.
[40] T.D. Culp, U. Hömmerich, J.M. Redwing, T.F. Kuech, K.L. Bray, J. Appl. Phys. 82 (1997) 368.

Materials Science and Engineering B105 (2003) 118–121

www.elsevier.com/locate/mseb

Synthesis and optical characterization of erbium-doped III-N double heterostructures

J.M. Zavada [a,*], J.Y. Lin [b], H.X. Jiang [b], P. Chow [c], B. Hertog [c], U. Hömmerich [d], Ei Ei Nyein [d], H.A. Jenkinson [e]

[a] *US Army Research Office, Durham, NC, USA*
[b] *Kansas State University, Manhattan, KS 66506, USA*
[c] *SVT Associates, Inc., Eden Prairie, MN 55344, USA*
[d] *Hampton University, Department of Physics, Hampton, VA 23668, USA*
[e] *US Army TACOM-ARDEC, Picatinny Arsenal, NJ 07806, USA*

Abstract

We report on the first successful synthesis of Er-doped III-N double heterostructures (DHs) grown on sapphire substrates. AlGaN layers, with an Al concentration of ∼12%, were prepared by metalorganic chemical vapor deposition and Er-doped GaN layers by molecular beam epitaxy. The Er concentration was estimated to be $\sim 10^{18}\,cm^{-3}$. GaN:Er/AlGaN single heterostructures (SHs) and AlGaN/GaN:Er/AlGaN DHs were studied using photoluminescence (PL) spectroscopy. Emission lines characteristic of the GaN:Er system (green: 537 and 558 nm, infrared: 1530 nm) were observed in all samples. With UV excitation, the infrared PL from the DHs showed a marked improvement compared to the SHs. The PL intensity increased and the spectra showed less defect-related emission. The enhanced PL properties may be due to more effective confinement of electron–hole pairs in the quantum well region.

PACS: 61.72; 71.55; 78.55; 78.66; 71.20

Keywords: Erbium; AlGaN; Double heterostructures; Quantum well; Luminescence

1. Introduction

Wilson et al. [1] were the first to observe optical emission from Er ions incorporated in III–V nitride semiconductors. GaN films were implanted with $Er^+ + O^+$ ions and then annealed at ∼650–700 °C. The Er densities were determined using secondary ion mass spectrometry (SIMS) analysis and the maximum Er density was on the order of $10^{19}\,cm^{-3}$ at a depth of ∼0.1 μm. Strong infrared luminescence, centered at 1.54 μm, was measured from the Er-implanted GaN samples using laser excitation at a wavelength of 457.9 nm. The spectra were centered at 1.54 μm and displayed many distinct lines indicative of the allowed transitions between the $^4I_{13/2}$ and the $^4I_{15/2}$ manifolds of the Er^{3+} 4f system. At room temperature, the integrated Er^{3+} luminescence intensity was more than 50% that at 77 K. However, ion implantation introduces considerable damage to the crystal host and post-implantation annealing was required to achieve any Er^{3+} luminescence.

Subsequently, MacKenzie et al. [2] succeeded in growing GaN films doped with Er atoms using a metalorganic molecular beam epitaxy (MOMBE) system with a solid elemental Er source and triethylgallium (TEGa) for the Ga flux. SIMS analysis of the Er-doped GaN layers indicated that Er densities in the 10^{19}–$10^{20}\,cm^{-3}$ range were achieved over a thickness from 0.5 to 1.0 μm. Later, Steckl and Birkhahn [3] and Birkhahn and Steckl [4] achieved in situ doping of GaN films using solid source MBE (SSMBE). The Er concentration in the GaN film reached $3 \times 10^{20}\,cm^{-3}$. These studies were expanded to yield GaN films doped with other rare earth elements such as Pr, Eu, and Tm [5].

Hömmerich et al. [6] compared the infrared luminescence properties of Er-doped GaN films grown by MOMBE and by SSMBE. Both types of samples displayed characteristic 1.54 μm PL resulting from the intra-4f Er^{3+} transitions. With below-gap excitation the samples exhibited very

* Corresponding author. Tel.: +1-919-5494238; fax: +1-919-5494310.
E-mail address: john.zavada@us.army.mil (J.M. Zavada).

0921-5107/$ – see front matter © 2003 Elsevier B.V. All rights reserved.
doi:10.1016/j.mseb.2003.08.028

similar 1.54 μm PL features and intensities. However, with above-gap excitation, very different PL features and intensities were found. The SSMBE samples exhibited a PL nearly 80 times more intense than that observed from the MOMBE sample. The infrared PL signal was exhibited very stable at temperatures as high as 550 K.

Since GaN has a bandgap of ∼3.51 eV, it should be possible to observe visible emission from higher excited 4f levels of the Er ions. Steckl and Birkhahn [3] were the first to measure such emission in GaN:Er films prepared by SSMBE [3]. With above-bandgap excitation, these films exhibited intense green PL for transitions from the $^2H_{11/2}$ and $^4S_{3/2}$ excited levels to the $^4I_{15/2}$ ground state. The visible luminescence spectra exhibited two primary lines located at 537 nm (2.309 eV) and 558 nm (2.222 eV). None of the GaN:Er films prepared by MOMBE exhibited green emission.

Following these early studies, there have been many efforts to improve the visible and infrared luminescence from GaN films doped with Er and other rare earth ions [7–9]. The demonstration of visible thin-film electroluminescence (TFEL) devices based on this class of materials has stirred wide spread interest for possible applications in full color displays [10]. Prime candidates for red-green-blue (RGB) emission are the rare earth ions Eu^{3+} (red), Er^{3+} (green), and Tm^{3+} (blue). A full-color TFEL phosphor system has been shown to yield high brightness (500–1000 cd/m^2) under direct current operation [11]. These studies have also shown that growth conditions significantly impact the Er^{3+} lattice location and the concentration of optically active Er^{3+} ions.

Here, we report on the first successful synthesis of GaN:Er/AlGaN heterostructures grown through a combination of metalorganic chemical vapor deposition (MOCVD) and molecular beam epitaxy on *c*-plane sapphire substrates. Characteristic visible and infrared emission lines of the GaN:Er system were observed in these samples, even for those with the thinnest Er-doped regions. With UV excitation the infrared PL signal from the double heterostructures (DHs) showed a marked improvement compared to the uncapped, single heterostructures (SHs).

2. Experimental details

The synthesis of the III-N heterostructures was achieved through a multi-stage growth process. First, AlGaN epilayers were grown by MOCVD on sapphire (0 0 0 1) substrates, as described elsewhere [11]. The n-type layers were ∼1 μm thick, with an Al content ∼12% and a Si doping ∼10^{18} cm^{-3}. This corresponds to a bandgap of ∼3.75 eV for the $Al_{0.12}Ga_{0.88}N$ alloy. Subsequently, GaN:Er epilayers were grown by MBE and had an Er concentration of ∼10^{18} cm^{-3} [12]. Two GaN:Er layer thicknesses were produced, 7 and 200 nm. After this stage, each sample was cut into two parts. One set was reserved for characterization, the other for a second growth of AlGaN by MOCVD. The top AlGaN layer was ∼200 nm thick, again with ∼12% Al.

PL spectra were measured using either the UV argon laser lines (336–363 nm) or a visible argon laser line at 496.5 nm. Infrared PL spectra were recorded using a 1-m monochromator equipped with a liquid-nitrogen cooled Ge detector. The visible PL measurements were made using a thermo-electric cooled photomultiplier tube for detection. The signal was processed using lock-in techniques or a boxcar averager. The obtained PL spectra were not corrected for the spectral response of the set-up.

3. Results and discussion

In Fig. 1 are shown the infrared PL spectra, measured at room temperature, for the 200 nm SH and the corresponding DH. The laser pump wavelength (λ_p) of 496.5 nm overlaps an intra-4f Er^{3+} absorption line ($^4I_{15/2} \rightarrow {}^4F_{9/2}$) [13]. The energy of the pump photons (2.48 eV) is below the bandgap of both the GaN and the $Al_{0.12}Ga_{0.88}N$ epilayers. As can be seen in Fig. 1, there is little difference in the two spectra. The main emission lines represent those from the Er^{3+} 4f system near 1.54 μm and 1.0 μm. The data indicate that there are optically active Er^{3+} ions in the GaN:Er epilayers and, that the absorption of the pump radiation in the top $Al_{0.12}Ga_{0.88}N$ layers in the DH was minimal. Furthermore, the MOCVD growth of the top layer did not significantly alter the optically activity of the Er^{3+} ions.

The data for the 7 nm SH and the corresponding DH were not as conclusive. The PL signals were weak and no distinct Er^{3+} emission lines could be observed. This may be due to the low excitation cross–section for the Er^{3+} ions under resonant pumping and the very thin Er-doped regions found in these samples.

The PL measurements using the UV lines at ∼336–363 nm yielded different results. The energy of the pump photons

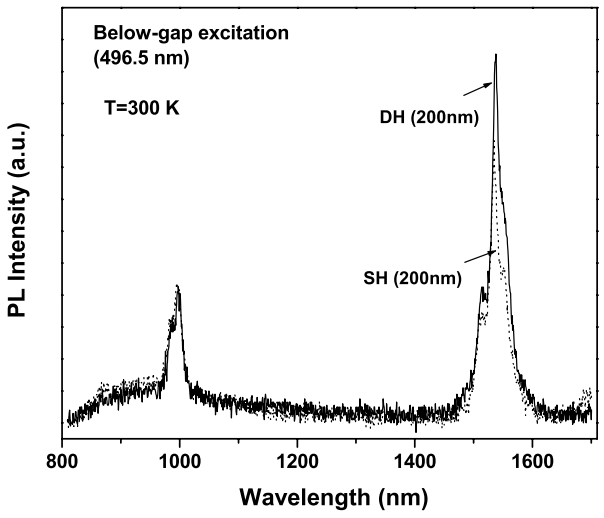

Fig. 1. Infrared PL spectra of a 200 nm GaN:Er/AlGaN SH (dotted line) and a 200 nm AlGaN/GaN:Er/AlGaN DH (solid line). The spectra were measured at 300 K using pump radiation at 496.5 nm.

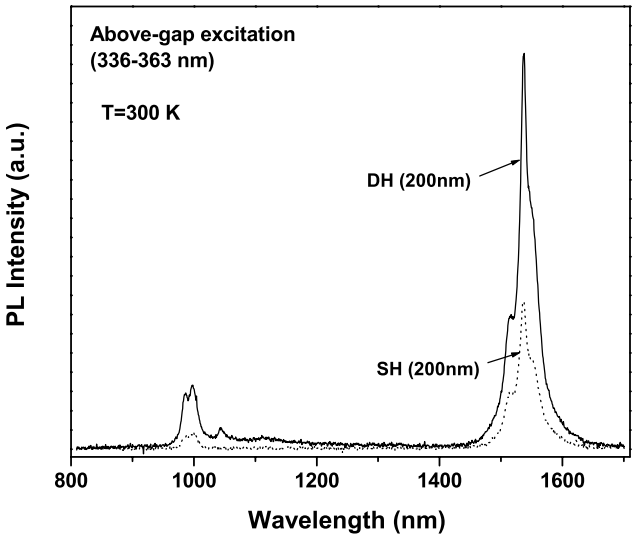

Fig. 2. Infrared PL spectra of a 200 nm GaN:Er/AlGaN SH (dotted line) and a 200 nm AlGaN/GaN:Er/AlGaN DH (solid line). The spectra were measured at 300 K using pump radiation at 336–363 nm.

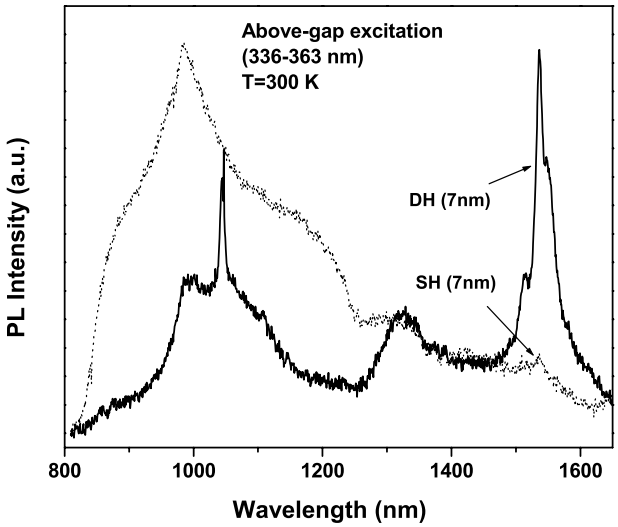

Fig. 3. Infrared PL spectra of a 7 nm GaN:Er/AlGaN SH (dotted line) and a 7 nm AlGaN/GaN:Er/AlGaN DH (solid line). The spectra were measured at 300 K using pump radiation at 336–363 nm.

(3.67–3.40 eV) is above the bandgap of the GaN epilayer, but below that of the $Al_{0.12}Ga_{0.88}N$ epilayer. In this case, the Er^{3+} ions are excited via electron–hole (e–h) pairs that are generated in the GaN:Er epilayer. In Fig. 2 are shown the infrared PL spectra for the 200 nm SH and the corresponding DH. While both spectra have features characteristic of the Er^{3+} system, the intensity from the DH is ∼3 times that from the SH. Since there may be some absorption of the pump radiation in the $Al_{0.12}Ga_{0.88}N$ cover layer, the actual increase of PL intensity in the DH may be even greater. The improved excitation efficiency of Er^{3+} in the DH seems to be due to better e–h confinement in the GaN:Er epilayer as a result of the band offsets with the $Al_{0.12}Ga_{0.88}N$ epilayers. Rather than recombining at the air-semiconductor interface as in the SH, the e–h pairs in the DH may have a greater probability of recombining near Er-related complexes. In addition, the top $Al_{0.12}Ga_{0.88}N$ epilayer reduces or eliminates surface recombination of the e–h pairs [14].

The data for the 7 nm SH and the corresponding DH also show an improvement with UV pumping. As shown in Fig. 3, the PL spectrum for the 7 nm SH is broad and not characteristic of Er^{3+} emission. The PL spectrum for the 7 nm DH has definite features of Er^{3+} emission near 1.54 μm. As in the case of the 200 nm DH, confinement of e–h pairs increases the transfer of energy to the Er^{3+} ions. The layer dimensions of the 7 nm DH are such that it is appropriate to use the term quantum well (QW) to describe this structure. With a well thickness of 7 nm and an Al content of 12%, quantum size effects are expected. This would likely lead to the Er ions experiencing a host region with a slightly higher bandgap and to an increase in the e–h lifetime. However, the main improvement in the PL signal appears to be due to a greater confinement of e–h pairs in the GaN:Er region.

The PL spectra for the two DHs are compared in Fig. 4. The spectra are quite similar except that the intensity from the 200 nm DH is ∼4 times greater than that from the 7 nm DH. It is surprising that the thicker DH did not yield a higher intensity comparer to the thinner one. For the UV wavelengths of 336–363 nm, the absorption coefficient for undoped GaN is $\sim 10^5\ cm^{-1}$ [15]. Assuming that the absorption for Er-doped GaN is at least as high, the intensity of the pump radiation is reduced by ∼86% before reaching the second interface of the 200 nm DH and by only ∼7% before reaching the second interface of the 7 nm DH. Consequently, since the generation of e–h pairs is dependent upon amount of absorbed radiation, the intensity from the 200 nm DH

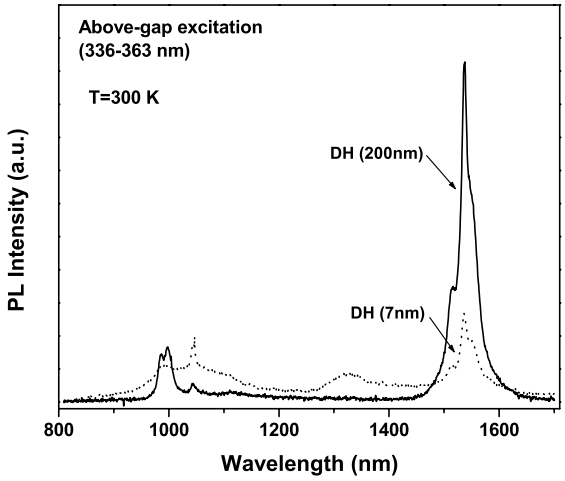

Fig. 4. Infrared PL spectra of two AlGaN/GaN:Er/AlGaN DHs measured at 300 K. The samples were excited with pump radiation at 336–363 nm. The GaN:Er layer was 7 nm in one (dotted line) and 200 nm thick in the other (solid line).

should be ~10–15 times greater than that from the 7 nm DH. The experimental result may be due to greater absorption of the pump radiation in the GaN:Er layer and to the closer proximity of the second heterojunction in the thinner sample.

4. Conclusions

There have been a few previous efforts to introduce rare earth ions in DH or QW regions. Sotta et al. reported on Er + O implantation into Si/SiO_2 quantum wells having a well thickness of 200 nm [16]. They found that the 1.54 μm emission at 10 K was 3–4 times more intense than that from similarly implanted bulk Si samples. Confinement of e–h pairs was cited as the physical mechanism leading to enhanced luminescence. Fujiwara et al. have studied luminescence from GaInP/GaAs:Er, O/GaInP DHs grown by MOCVD. They found the PL intensity at 4.2 K from the DHs was ~3 times higher than that from a SH [14]. They also processed the structures into light emitting diodes (LEDs) measured strong room temperature Er^{3+} luminescence under forward bias [17].

With wide bandgap semiconductors, Lozykowski et al. reported on the implantation of Eu into an AlGaN/GaN superlattice (SL) [18]. Well thickness in the SL was 4 nm and barrier thickness was 6 nm. Post-implantation annealing was needed to achieve emission from the Eu^{3+} centers. Room temperature luminescence at 622 nm was 58% more intense than that from similarly implanted GaN thin film samples. However, due to the implantation, the Eu ions were located in the AlGaN barriers as well as in the GaN wells. It is difficult to conclude from their experiments that e–h confinement was responsible for the enhancement. In the present set of experiments, it is more certain that the Er^{3+} ions are located in a single GaN epilayer and that the enhanced luminescence at RT is due to better e–h confinement and reduced surface recombination. The use of MOCVD and MBE growth techniques has permitted the synthesis of precise multilayer SHs and DHs. Such structures are the basic building blocks that can be used to form true Er-doped, AlGaN/GaN p–n LEDs in the future.

Acknowledgements

The work at Hampton Univ. and Kansas State University was partially supported by the ARO.

References

[1] R.G. Wilson, R.N. Schwartz, C.R. Abernathy, S.J. Pearton, N. Newman, M. Rubin, T. Fu, J.M. Zavada, Appl. Phys. Lett. 65 (8) (1994) 992–994.
[2] J.D. MacKenzie, C.R. Abernathy, S.J. Pearton, U. Hömmerich, J.T. Seo, R.G. Wilson, J.M. Zavada, Appl. Phys. Lett. 72 (1998) 2710.
[3] A. Steckl, R. Birkhahn, Appl. Phys. Lett. 73 (1998) 1702.
[4] R. Birkhahn, A.J. Steckl, Appl. Phys. Lett. 73 (1998) 2143.
[5] A.J. Steckl, J.M. Zavada, MRS Bull. 24 (9) (1999) 33.
[6] U. Hömmerich, J.T. Seo, J.D. MacKenzie, C.R. Abernathy, R. Birkhahn, A.J. Steckl, J.M. Zavada, MRS Fall 1999 Meeting, Paper W11.65.
[7] G.S. Pomerenke, P.B. Klein, D.W. Langer (Eds.), Proceedings of the Materials Research Society on Rare Earth Doped Semiconductors I, vol. 301, 1993.
[8] S. Coffa, A. Polman, R.N. Schwartz (Eds.), Proceedings of the Materials Research Society on Rare Earth Doped Semiconductors II, vol. 422, 1996.
[9] J. Zavada, T. Gregorkiewicz, A.J. Steckl (Eds.), Proceedings of E-MRS Symposium on Rare Earth Doped Semiconductors III, Spring 2000, Mater. Sci. Eng. B 81 (2001).
[10] A.J. Steckl, J. Heikenfeld, D.S. Lee, M.J. Garter, C.C. Baker, Y. Wong, R. Jones, IEEE J. Sel. Top. Quant. 8 (2002) 749.
[11] J. Li, K.B. Nam, M.C. Nakarmi, J.Y. Lin, H.X. Jiang, Appl. Phys. Lett. 81 (2002) 3365.
[12] SVT Associates, Inc., unpublished.
[13] G.H. Dieke, Spectra and Energy Levels of Rare Earth Ions in Crystals, Wiley, New York, 1968.
[14] A. Koizumi, N. Watanabe, K. Inoue, Y. Fujiwara, Y. Takeda, Physica B 308–310 (2001) 891.
[15] C.H. Yan, W.H. Yao, J.M. Van Hove, A.M. Wochak, P.P. Chow, J.M. Zavada, J. Appl. Phys. 88 (2000) 3463.
[16] D. Sotta, V. Calvo, H. Ulmer-Tuffigo, N. Magnea, E. Hadji, F. Fournel, J.L. Rouviere, D. Jalabert, H. Moriceau, B. Aspar, Mater. Sci. Eng. B 81 (2001) 43.
[17] Y. Fujiwara, A. Koizumi, Y. Takeda, European Materials Society Spring Meeting 2003, Strasbourg, France, Paper J-III.5.
[18] H.J. Lozykowski, W.M. Jadwisienczak, J. Han, I.G. Brown, Appl. Phys. Lett. 77 (2000) 767.

phys. stat. sol. (c) **2**, No. 7, 2796–2799 (2005) / **DOI** 10.1002/pssc.200461467

Spectroscopic studies of the infrared emission from Tm doped $Al_xGa_{1-x}N$ thin films

E. Nyein[1], **U. Hömmerich**[*1], **D. S. Lee**[2], **A. J. Steckl**[2], and **J. M. Zavada**[3]

[1] Department of Physics, Hampton University, Hampton, Virginia 23668, USA
[2] Nanoelectronics Laboratory, University of Cincinnati, Cincinnati, Ohio 45221, USA
[3] US Army Research Office, Durham, North Carolina 27709, USA

Received 12 July 2004, accepted 7 February 2005
Published online 1 April 2005

PACS 78.55.Cr

The infrared (IR) emission properties of in-situ Tm doped $Al_xGa_{1-x}N$ thin films ($0 \le x \le 1$) prepared by solid-source molecular-beam epitaxy were investigated. All samples exhibited 1.48 μm photoluminescence (PL) from the $^3H_4 \rightarrow {}^3F_4$ transition of Tm^{3+}. The absolute intensity of the 1.48 μm PL varied strongly with Al content and reached a maximum for $Al_{0.81}Ga_{0.19}N$:Tm. The integrated 1.48 μm PL from $Al_{0.81}Ga_{0.19}N$:Tm was weakly temperature dependent and decreased by less than a factor of two between 15 K and 300 K. The PL lifetime of the $^3H_4$ state decreased only slightly from ~102 μs to ~86 μs for the same temperature range. The results suggest that non-radiative decay processes in the $^3H_4$ level are small in $Al_{0.81}Ga_{0.19}N$:Tm, which is supported by the well-known energy-gap law for multiphonon relaxations.

1 Introduction

In recent years rare-earth (RE) doped semiconductors have received significant attention because of possible applications in display technology, lasers, and optical communications [1]. Earlier work on infrared studies of RE doped semiconductors was mainly focused on the 1.54 μm emission from Er^{3+} ions due to the overlap with the minimum loss window of silica based fibers. The growing demand for increased bandwidth of optical communication systems has prompted efforts to study the IR emission from other RE ions such as Dy^{3+} (1.3 μm), Pr^{3+} (1.3, 1.6 μm), Nd^{3+} (1.3 μm), and Tm^{3+} (1.48 μm). Tm^{3+} is currently considered the most promising candidate for S-band optical amplifiers, which cover a wavelength range from 1450 to 1530 nm [2].

Tm^{3+} doped insulators exhibit an IR emission band at ~ 1.48 μm from the $^3H_4 \rightarrow {}^3F_4$ transition [3–5]. There are several drawbacks inherent to this transition of Tm^{3+}. The first problem relates to the Tm^{3+} concentration and possible cross-relaxation among Tm^{3+} ions (see Fig. 1). During this process, an excited Tm^{3+} ion decays from the $^3H_4$ state and transfers its energy to another Tm^{3+} ion in the $^3H_6$ ground state. Consequently, both ions end up in the $^3F_4$ level ($^3H_4$,$^3H_6 \rightarrow {}^3F_4$,$^3F_4$), which reduces the 1.48 μm PL intensity and leads to enhanced emission at ~1.8 μm. Therefore, the Tm^{3+} concentration has to be carefully optimized to reduce the effect of cross-relaxation [3–5]. Moreover, the 1.48 μm Tm^{3+} PL has a self-terminating nature since the lifetime of the upper level $^3H_4$ is shorter than that of the lower $^3F_4$ level This difficulty can be overcome by using upconversion pumping schemes or co-doping with Ho^{3+} or Tb^{3+} [3,4].

[*] Corresponding author: e-mail: uwe.hommerich@hamptonu.edu

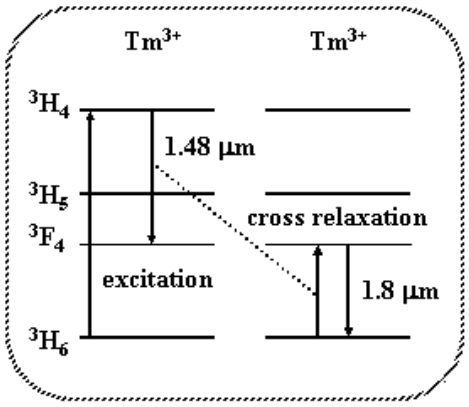

Fig. 1 Schematic energy-level diagram of Tm^{3+} indicating cross-relaxation processes.

Finally, the $^3H_4$ level can decay non-radiatively to the lower lying $^3H_5$ level, which results in a low emission efficiency of the 1.48 μm PL. Therefore, Tm^{3+} hosts for optical communications applications have been restricted to low phonon energy hosts, which provide a low probability for multiphonon relaxation [3-5]. So far, very little attention has been paid to $^3H_4 \rightarrow {}^3F_4$ transition in Tm^{3+} doped semiconductors [1]. In this paper we report on the 1.48 μm PL properties of $Al_xGa_{1-x}N$:Tm films as a function of host composition and temperature.

2 Experimental details

Tm doped $Al_xGa_{1-x}N$ films were grown on *p*-type (111) Si substrates by solid-source molecular beam epitaxy with various Al compositions: x =0 (GaN), 0.16, 0.29, 0.39, 0.62, 0.81, and 1 (AlN). The Tm cell temperature was ~600 ºC resulting in Tm concentrations between ~0.2 and ~0.5 at.%. The details of the material preparation were previously reported [6]. PL spectra were measured using the UV laser lines (333.6-363.8) nm of an Argon laser for excitation. The PL lifetime was measured using a Nd:YAG pumped Optical Parametric Oscillator (OPO) system (10 ns pulses, 10 Hz repetition rate). For temperature dependent PL measurements, the sample was mounted on the coldfinger of a two-stage closed-cycle helium refrigerator. The PL signal was focused into a 1-m monochromator and detected using a liquid nitrogen cooled Ge detector in combination with standard lock-in technique. The PL decay transients were monitored at ~800 nm using a photomultiplier tube and the signal was averaged on a digital oscilloscope.

3 Results and discussion

Figures 2a and b show the room temperature IR PL spectra of Tm doped $Al_xGa_{1-x}N$ films with varying Al content. The corresponding bandgap energies are given in the figure. The PL spectra were measured using the UV Argon laser lines (333.6-363.8) nm, which corresponds to below-gap excitation for $Al_xGa_{1-x}N$ samples with x > 0 and above-gap pumping for x = 0 (GaN). IR emission bands centered around 1.2 μm, 1.48 μm, and 1.7 μm were observed, which can be assigned to the intra-4f transitions $^3H_5 \rightarrow {}^3H_6$, $^3H_4 \rightarrow {}^3F_4$, and $^3F_4 \rightarrow {}^3H_6$ of Tm^{3+} ions, respectively [3–5]. It was noticed that the 1.48 μm PL intensity (Fig. 2a) and spectral features (Fig. 2b) varied with Al contents in $Al_xGa_{1-x}N$: Tm. The strongest IR emission at ~ 1.48 μm ($^3H_4 \rightarrow {}^3F_4$) was observed from $Al_{0.81}Ga_{0.19}N$:Tm with a linewidth of ~ 110 nm at full-width half maximum (FWHM). In comparison, typical emission linewidths reported for the 1.54 μm emission from Er^{3+} ions range from 30-50 nm [1,3].

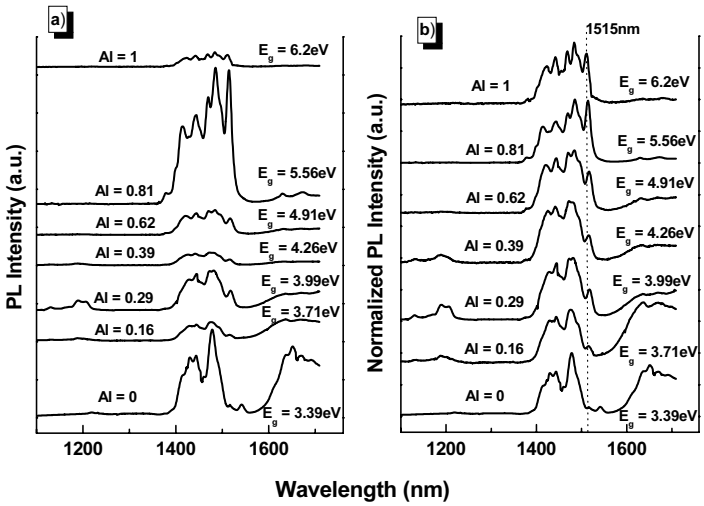

Fig. 2 a) Infrared PL spectra of $Al_xGa_{1-x}N$:Tm films at 300 K showing the intensity changes as a function of Al content . b) Normalized IR PL of $Al_xGa_{1-x}N$:Tm for direct comparison of spectral changes. The dotted line indicates the position of the 1515 nm PL line.

It is interesting to note that a new PL line located at ~1515 nm gained in intensity with increasing Al content (Fig. 2 b). The 1515 nm PL could indicate changes in the crystal field splittings of Tm^{3+} ions for different host compositions. It is also possible that this IR emission line arises from transitions between higher excited states of Tm^{3+} such as $^1G_4 \rightarrow {}^3F_2$, $^3F_3$ or $^1D_2 \rightarrow {}^1G_4$ [3]. With increasing bandgap of $Al_xGa_{1-x}N$: Tm, the $^1G_4$ and $^1D_2$ states shift within the bandgap of the host and participate more effectively in the emission process [6,7]. Several researchers have studied the IR emission from Tm doped materials using Judd-Ofelt analysis and reported branching ratios of less than ~1% for the $^1D_2 \rightarrow {}^1G_4$ and $^1G_4 \rightarrow {}^3F_2$ transitions [8,9]. A slightly higher branching ratio of ~3% has been reported for the $^1G_4 \rightarrow {}^3F_3$ transition, which makes this transition the most likely candidate for the 1515nm line. More detailed spectroscopic studies on the identification of the 1515nm PL are still in progress.

The infrared emission at 1.48 μm of Tm doped $Al_{0.81}Ga_{0.19}N$ was measured in the temperature range from 15 to 300 K as shown in Fig. 3a. It was observed the integrated 1.48 μm PL intensity decreased by less than a factor of two between 15 K and 300 K. The PL lifetime of the $^3H_4$ excited state was measured by pumping resonantly into the $^1G_4$ level at ~479 nm and monitoring the emission at ~800 nm through the $^3H_4 \rightarrow {}^3H_6$ transition (see insert of Fig. 3b. The PL lifetime of $^3H_4$ state decreased from ~ 102 μs to ~ 86 μs between 15 K and 300 K, which suggests that nonradiative multiphonon processes are small. Assuming the PL decay of $^3H_4$ state is purely radiative at 15 K, the 1.48 μm emission efficiency can be estimated to be ~ 80% at 300 K. The high emission efficiency of the $^3H_4$ level in $Al_{0.81}Ga_{0.19}N$:Tm AlGaN:Tm is consistent with the energy-gap law for multiphonon relaxations, which is given by the following expression [3]:

$$W_{nr} = \alpha \cdot e^{-\beta \frac{\Delta E}{\hbar \omega}} \tag{1}$$

where W_{nr} is the nonradiative decay rate, α and β are host dependent parameters, ΔE is the energy gap between the RE states of interest, $\hbar\omega$ is the highest phonon energy. According to equation (1), the lower the maximum phonon energy of the host, the more phonons are required to bridge the energy gap ΔE between two RE levels. Therefore, nonradiative decay processes are less likely to occur in low-phonon hosts. For AlGaN: Tm, the energy gap between $^3H_4$ and $^3H_5$ level was estimated to be ~ 4080 cm^{-1}. The maximum phonon energies for GaN: Tm and AlN are ~ ~750 cm^{-1} and ~900 cm^{-1}, respectively [10]. The number of phonons related to the energy-gap law can then be estimated to be ~ 4.6-5.4, which is comparable to results reported for Tm doped tellurite glasses [4]. The 1.48 μm emission efficiency in Tm doped telluride glass was determined to be near unity [4]. Based on the energy gap law, nonradiative decay processes for the $^3H_4$ in AlGaN: Tm are expected to play only a minor role.

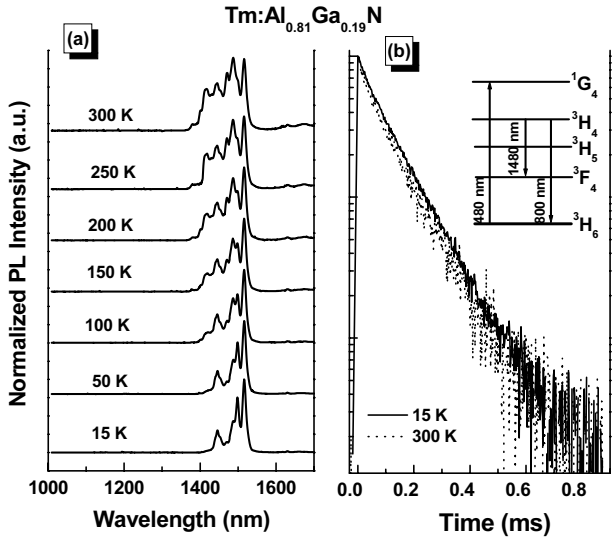

Fig. 3 a) Infrared PL spectra of $Al_{0.81}Ga_{0.19}N$:Tm over a temperature range from 15-300 K. The PL spectra were measured under UV Argon laser excitation (333.6-363.8) nm. b) Temperature dependent PL decay curves monitored at 808 nm. A partial energy level diagram of Tm^{3+} is also shown.

4 Conclusions

We reported on the IR emission characteristics of $Al_xGa_{1-x}N$: Tm films grown by solid-source MBE. All samples showed characteristic 1.48 μm PL from the $^3H_4 \rightarrow {}^3F_4$ transition of Tm^{3+}. The strongest 1.48 μm emission was observed from $Al_{0.81}Ga_{0.19}N$: Tm with a bandwidth ~ 110 nm. Temperature dependent PL studies revealed a high emission efficiency of 1.48 μm PL, consistent with predictions derived from the energy-gap law. The initial studies indicate the potential of AlGaN: Tm films for electroluminescence device applications in the S-band optical communcations window.

Acknowledgements The work at H.U. was supported through ARO grant DAAD19-02-1-0316. The work at U. C. was supported by ARO grant DAAD 19-99-1-0348.

References

[1] Rare Earth Doped Materials for Photonics, Proceedings of E-MRS Symposium, Spring 2003 (P. Ruterana, Editor.), Mater. Sci. Eng. B **105**, Elsevier (2003).
[2] M. Yamada and M. Shimizu, NTT Technical Rev. **1**, 80 (2003).
[3] A. A. Kaminskii, Crystalline Lasers: Physical Processes and Operating Schemes, CRC Press, New York, 1996.
[4] E. R. Taylor, Li Na Ng, and Neil P. Sessions, J. Appl. Phys. **92**, 112 (2002).
[5] J. Ganem, J. Crawford, P. Schmidt, N. W. Jenkins, and S. R. Bowman, Phys. Rev. B **66**, 245101 (2002).
[6] D. S. Lee and A. J. Steckl, Appl. Phys. Lett. **83** (11), 2094 (2003).
[7] U. Hömmerich, E. Nyein, D. S. Lee, A. J. Steckl, and J. M. Zavada, Appl. Phys. Lett. **83**, 4556 (2003).
[8] W. Romanowski, S. Golab, I. Sokolska, G. Dominiak-Dzik, M. Berkowski, J. Fink-Finowicki, M. Baba, Appl. Phys. B **68**, 199 (1999).
[9] G. Ozen, A. Kermaoui, J. P. Denis, X. Wu, F. Pelle, and B. Blanzat, J. Lumin. **63**, 85 (1995).
[10] http://www.ioffe.ru/SVA/NSM/Semicond/GaN/index.html

Excitation-Wavelength Dependent and Time-Resolved Photoluminescence Studies of Europium Doped GaN Grown by Interrupted Growth Epitaxy (IGE)

Ei Ei Nyein[1], Uwe Hömmerich[1,*], Chanaka Munasinghe[2], Andrew J. Steckl[2], and John M. Zavada[3]
[1]Department of Physics, Hampton University, Hampton, VA 23668
[2]Department of Electrical and Computer Engineering, University of Cincinnati, OH 45221
[3]U.S. Army Research Office, Research Triangle Park, NC 27709
*E-mail: uwe.hommerich@hamptonu.edu

ABSTRACT

The emission properties of Eu doped GaN thin films prepared by interrupted growth epitaxy (IGE) were investigated through excitation-wavelength dependent and time-resolved photoluminescence (PL) studies. Under above-gap excitation (333-363 nm) large differences were observed in the Eu^{3+} PL intensity and spectral features as a function of Ga shutter cycling time. The overall strongest red Eu^{3+} PL intensity was obtained from a sample grown with a Ga-shutter cycling time of 20 minutes. The main Eu^{3+} emission line originating from $^5D_0 \rightarrow {}^7F_2$ transition was composed of two peaks located at 620 nm and 622 nm, which varied in relative intensity depending on the growth conditions. The room-temperature emission lifetimes of the samples were non-exponential and varied from ~50 μs to ~200 μs (1/e lifetimes). Under resonant excitation at 471 nm ($^7F_0$->$^5D_2$) all samples exhibited nearly identical PL spectra independent of Ga shutter cycling time. Moreover, the Eu^{3+} PL intensities and lifetimes varied significantly less compared to above-gap excitation. The excitation wavelengths dependent PL results indicate the existence of different Eu^{3+} centers in GaN: Eu, which can be controlled by the Ga shutter cycling time.

INTRODUCTION

Rare-earth (RE) doped III-V compound semiconductors have received significant attention due to their applications in light emitting devices and for their unique optical and electrical characteristics [1,2]. In recent years, RE ions have been introduced into GaN for optoelectronic devices operating in the ultraviolet (UV), visible, and infrared (IR) spectral region [1,2]. Eu^{3+} doping of GaN has been of particular interest because of its efficient red emission at ~ 622 nm used in electroluminescence (EL) devices [2]. In addition, Eu^{3+} exhibits a relatively simple energy diagram, which makes Eu^{3+} an excellent spectroscopic probe [3-5]. The ground state level $^7F_0$ and the lowest emitting level $^5D_0$ of Eu^{3+} are non-degenerate. Therefore, the optical transition $^5D_0 \rightarrow {}^7F_0$ can provide important information on different Eu^{3+} centers in the GaN lattice.

The main aim of this research is to develop compact, efficient, and bright EL devices based on RE doped GaN thin films. To achieve this goal, the materials need to be optimized for several growth parameters: e.g. RE concentration, growth temperature, and III/V ratio. In this work, a set of GaN:Eu samples was prepared by a new growth technique called “Interrupted Growth Epitaxy” (IGE) [6]. During IGE the group III (Ga) shutter is closed for a certain time interval, which allows the GaN: Eu film to compensate for any nitrogen deficiency. Improvements in the GaN: Eu EL device performance by more then an order of magnitude were

observed from GaN: Eu films grown by IGE compared to conventional MBE [6]. Initial studies of the photoluminescence (PL) properties of these samples are presented in this paper.

EXPERIMENTAL PROCEDURES

IGE was recently developed at the University of Cincinnati in order to determine the optimum group V/III growth ratio for GaN: Eu. Closing the Ga shutter for a certain time interval allows the GaN:Eu film to compensate for any nitrogen deficiency. A set of Eu doped GaN films with group III (Ga) shutter open times of 5, 10, 15, 20, 30, and 60 min were grown using IGE technique on Si substrates. A full growth run of Eu doped GaN covered a time period of 60 minutes. For the main growth, the substrate temperature was ramped to 650 °C and the Ga cell temperature was 900 °C. The Eu cell temperature was 440 °C, resulting in an estimated Eu concentration of ~0.1 at. % [6].

PL measurements were performed using the UV argon laser line (333.6-363.8) nm for above-gap excitation. Resonant pumping into the $^7F_0 \rightarrow {}^5D_2$ Eu^{3+} transition at ~ 471 nm was obtained using the output of a Nd:YAG pumped Optical Parametric Oscillator (OPO) system. For temperature-dependent PL measurements, the sample temperature was controlled between 15 K and 300 K using a two-stage closed-cycle helium refrigerator. The visible luminescence was analyzed by a 0.5 or 1-m monochromator and detected with a thermo-electric cooled photomultiplier tube (PMT). PL lifetime data were taken with the third harmonic output of a pulsed Nd:YAG laser (355-nm) for above-gap excitation and the OPO system operating at ~ 471 nm for resonant excitation. The luminescence signal was processed using either a lock-in amplifier or a boxcar averager and PL decay curves were recorded using a digitizing oscilloscope.

RESULTS AND DISCUSSION

Above-gap emission spectra and PL decay

Figure 1 shows an overview of the room-temperature PL spectra of Eu doped GaN for various Ga shutter cycling times. The PL was excited using an UV argon laser (333.6-363.8 nm), which corresponds to above-gap pumping. The characteristic Eu^{3+} red emission at ~ 622 nm attributed to the intra-4f $^5D_0 \rightarrow {}^7F_2$ transition was observed in all samples accompanied by other Eu^{3+} lines at ~ 601 nm ($^5D_0 \rightarrow {}^7F_1$) and ~ 663 nm ($^5D_0 \rightarrow {}^7F_3$). The strongest red emission was observed from GaN:Eu with a shutter cycling time of 20 min as illustrated in Fig. 1 (a). The integrated PL intensity as a function of Ga shutter cycling time is also depicted in Fig. 1 (b).

It can be noticed from Fig. 1, that the main red emission line consisted of two peaks at ~ 620 nm and ~ 622 nm. The intensity ratio of these two PL lines changed as a function of Ga shutter cycling time. The GaN:Eu sample with the strongest Eu^{3+} PL intensity exhibited mainly emission from the 620 nm PL line. The observation of two strong $^5D_0 \rightarrow {}^7F_2$ PL lines suggests the existence of two dominant Eu^{3+} sites (labeled in the following as site 1 and site 2). It is also interesting to note that the PL line at ~ 633 nm was unusually pronounced in some GaN:Eu samples, and was correlated with the 620 nm PL line intensity. The weak emission lines at 583, 586, and 589 nm are most probable due to $^5D_0 \rightarrow {}^7F_0$ transitions further indicating the existence of different Eu^{3+} centers in GaN:Eu samples grown by IGE technique [6].

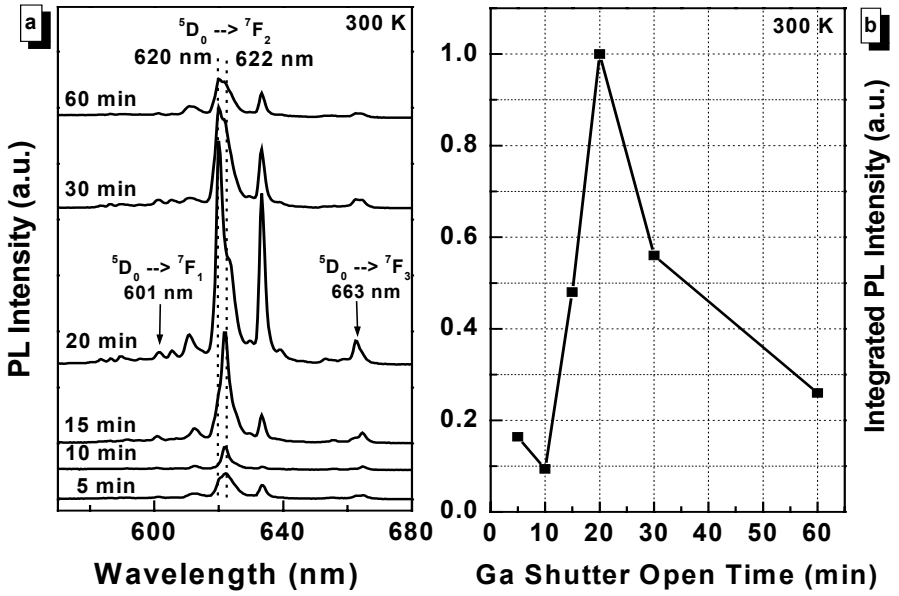

Figure 1. (a) Room temperature PL spectra of GaN:Eu films under above-gap excitation. The group III shutter open times are also indicated in the graph. (b) Integrated PL intensity of GaN:Eu films as a function of Ga/Eu shutter cycling time.

The room temperature PL decay transients under above-gap excitation are shown in Fig. 2. It can be noted that the PL lifetimes varied significantly between the samples. The PL decay transient of the strongest emitting sample (20 min) showed a 1/e lifetime value of only ~54 μs.

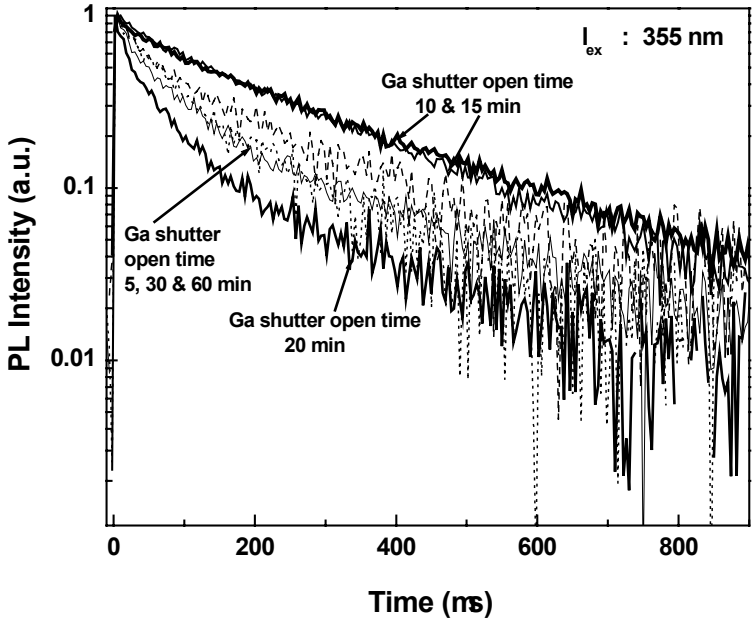

Figure 2. PL decay transients of GaN:Eu films under above-gap excitation (355 nm) at 300 K.

The PL decays of GaN:Eu films with Ga shutter cycling times of 10 and 15 min were nearly exponential with 1/e lifetime values of ~ 208 μs. The 5, 30, and 60 min samples, which have both Eu^{3+} sites, showed PL lifetimes between ~ 75 μs and ~120 μs. The PL decay measurements indicate that Eu^{3+} site 1 (PL peak: ~ 620 nm) has a "short" lifetime of ~ 54 μs and Eu^{3+} site 2 (PL peak: ~ 622 nm) possesses a "long" lifetime of ~ 208 μs.

Figure 3 depicts the temperature dependent PL lifetimes for samples with Ga shutter cycling times of 20 and 10 min. The PL lifetime of the 20 min sample exhibited a large change in lifetime between 15 K and 300 K, as shown in Fig. 3 (a). The 1/e PL lifetime values at 15 K and 300 K were ~ 158 μs and ~ 54 μs, respectively, which shows a ~ 66 % decrease relative to its low temperature value. On the other hand, the PL lifetimes were nearly temperature independent for the GaN:Eu sample with a Ga shutter time of 10 min. For this sample the lifetime decreased by only ~ 17 % relative to its low temperature value [see Fig. 3 (b)]. The large difference in the decay time behavior provides further support for the existence of different Eu^{3+} sites in these samples.

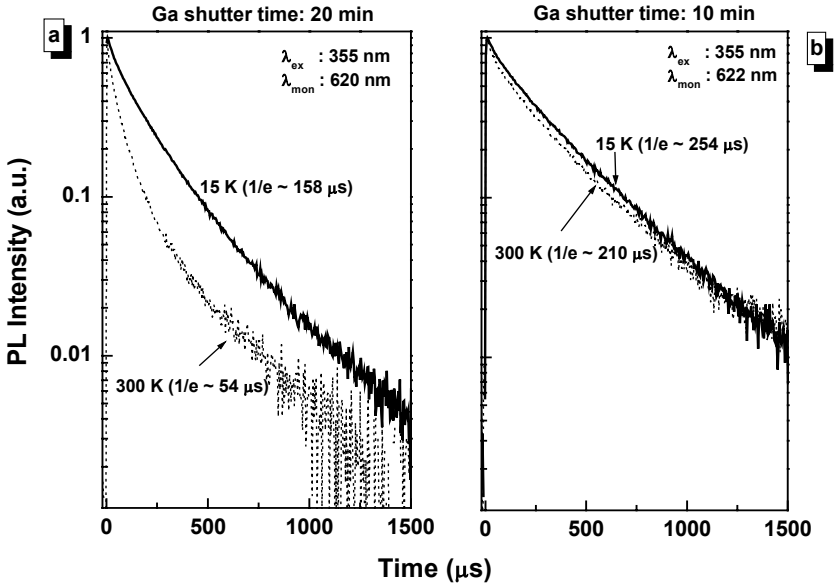

Figure 3. Temperature dependent PL decay transients for the samples with Ga shutter time (a) 20 min and (b) 10 min under above-gap excitation. The 1/e lifetime values are also indicated in the graph.

Below-gap emission Spectra and PL decay

To gain more insight in the Eu^{3+} PL properties of GaN:Eu prepared by IGE, PL spectra were recorded under resonant intra-4f Eu^{3+} excitation using the 471nm output of an OPO system [Fig. 4 (a)]. Nearly identical Eu^{3+} PL spectra with the $^5D_0 \rightarrow {}^7F_2$ emission line at ~ 622 nm were observed for all samples. This observation suggests that Eu^{3+} site 2 is dominant under resonant pumping. The normalized PL spectra under above-gap excitation are shown in Fig. 4 (b) for comparison.

The differences in PL spectra under above-gap and resonant-excitation further indicate that different Eu^{3+} centers were formed in GaN during the IGE growth process. Compared to above- gap excitation, resonant Eu^{3+} excitation preferentially excites only one Eu^{3+} site (site 2).

The PL decay monitored at ~ 622 nm under resonant-excitation showed that the transients are nearly exponential with variations in 1/e lifetimes ranging from ~ 100-215 μs.

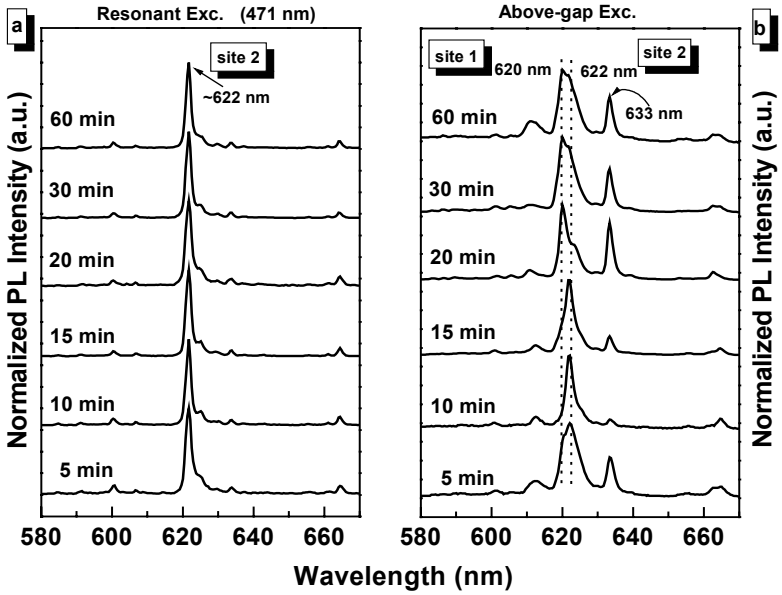

Figure 4. Normalized PL spectra of GaN: Eu under (a) resonant and (b) above-gap excitation. The group III shutter open times during IGE growth are also indicated in the graph.

PL excitation measurements

We recently studied the incorporation of Eu^{3+} ions in GaN: Eu films grown by conventional solid-source MBE (SSMBE) technique and identified at least five Eu^{3+} centers [5]. Initial PL excitation (PLE) studies at room-temperature were performed on GaN: Eu samples grown by IGE technique as shown in Fig. 5.

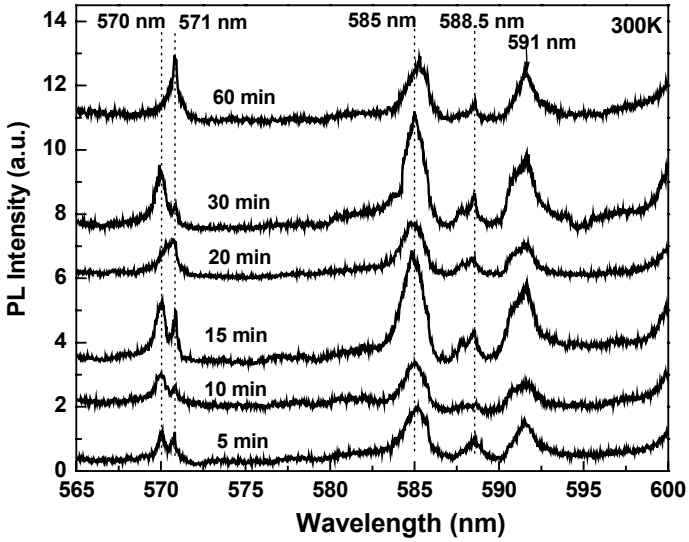

Figure 5. Room temperature PLE spectra of GaN:Eu films with various Ga shutter cycling time.

The Eu^{3+} luminescence was monitored at ~ 622 nm and the excitation wavelength was scanned in the spectral region of the $^7F_0 \rightarrow {}^5D_0$ transition between 565 and 600 nm. Interestingly, the observed PLE spectra were similar to the results obtained from GaN:Eu grown by SSMBE [5]. Three main PLE peaks were observed at ~ 571, 585, and 588.5 nm from all samples. For some samples the ~571 nm lines exhibited a splitting into two lines. The PLE line at 591 nm does not originate from the $^7F_0$ ground state, as previously reported [5]. The obtained PLE spectra further demonstrate the existence of different Eu^{3+} centers in the GaN:Eu samples prepared by IGE growth. An attempt was made to selectively excite the different Eu^{3+} centers using the tunable laser output from an OPO system. However, due to a poor signal to noise ratio, no spectral differences were observed. Further site-selective PL spectroscopy is needed to elucidate the incorporation of different Eu^{3+} sites in GaN sample grown by IGE technique.

SUMMARY

Spectroscopic results on the emission properties were presented on a set of GaN:Eu films grown by interrupted growth epitaxy (IGE). The strongest Eu^{3+} red emission under above-gap excitation was observed for a sample with a 20 min Ga cycling time. Two Eu^{3+} sites with the $^5D_0 \rightarrow {}^7F_2$ PL peaks located at 620 nm (site 1) and 622 nm (site 2) were dominant in the above-gap PL spectra. It was found that Eu^{3+} site 1 exhibited a "short" lifetime (~ 54 μs) and Eu^{3+} site 2 had a "long" lifetime (~ 208 μs). Contrary to above-gap excitation, resonant Eu^{3+} excitation selectively excited only one Eu^{3+} center (site 2). PLE measurement in the $^7F_0 \rightarrow {}^5D_0$ spectral region provided further supported for the different Eu^{3+} centers in these samples. Additional high-resolution PL and site-selective PL studies are required for these samples to obtain a better understanding of the incorporation of Eu^{3+} ions into GaN. Also, efforts to relate the Eu^{3+} PL properties to the crystalline quality of GaN: Eu samples grown by IGE are still in progress.

ACKNOWLEDGEMENTS

The authors from Hampton University would like to acknowledge financial support by ARO grant DAAD19-02-1-0316. The work at University of Cincinnati was supported by ARO grant DAAD19-03-1-0101.

REFERENCES

1. *Rare Earth Doped Materials for Photonics,* Proceedings of E-MRS Symposium Spring 2003, (P.Ruterana, Editor.), Mater. Sci. Eng. **B105**, Elsevier (2003).
2. A. J. Steckl, J. C. Heikenfeld, D. S. Lee, M. J. Garter, C. C. Baker, Y. Wang, R. Jones, IEEE J. Sel. Top. Quant. Electronics **8**,749 (2002).
3. T. Monteiro, C. Boemare, M. J. Soares, R. A. Sa Ferreira, L. D. Carlos, K. Lorenz, R. Vianden, E. Alves, *Physica B* **308-310**, 22-25 (2001).
4. Ei Ei Nyein, U. Hömmerich, J. Heikenfeld, D. S. Lee, A. J. Steckl, and J. M. Zavada, *Appl. Phys. Lett.* **82**, 1655-1657 (2003).
5. U. Hömmerich, E. E. Nyein, D. S. Lee, J. Heikenfeld, A. J. Steckl, and J. M. Zavada, *Mater. Sci. & Eng.* **B105**, 91-96 (2003).
6. C. Munasinghe and A. J. Steckl, *Proceedings of the International Electroluminescence Conference*, Toronto, Canada, September 2004, pp.341-343.